

Diploma thesis

The role of the NKG2D receptor during infection with *Helicobacter pylori*

submitted by

Sebastian Edmund WRIGHTON

for the academic degree of

Doctor of Medicine

(Dr. med. univ.)

at the

Medical University of Graz

Institute of Pathology

under the supervision of

Univ.-Prof. Dr. med. univ. Gregor GORKIEWICZ

Graz, 01.03.2018

Eidesstattliche Erklärung

Ich erkläre ehrenwörtlich, dass ich die vorliegende Arbeit selbstständig und ohne fremde Hilfe verfasst habe, andere als die angegebenen Quellen nicht verwendet habe und die den benutzten Quellen wörtlich oder inhaltlich entnommenen Stellen als solche kenntlich gemacht habe.

Graz, am 01.03.2018

Sebastian Edmund Wrighton, eh

Acknowledgments

I would like to thank my supervisor Professor Gregor Gorkiewicz, not only for his patient and thoughtful guidance through the process of creating this diploma thesis. I am extremely grateful as it was he, who by welcoming me into his research group allowed me to see the wonderful nature of science and research in a broader sense. In doing so, he awakened in me a dream to one day become a scientist as well.

I would also like to thank my colleagues from the research group. Because of them I was never lacking useful and insightful input and they always made it a pleasure to work in the lab. I am honoured to call them my friends. In this regard, I would especially like to thank my colleague Margit Neger, as without her help, assistance, and patient teaching this diploma thesis would never have been possible.

I would like to thank my family for always being extremely loving, supportive, and patient, even when times were hard. If it weren't for them, I certainly would not have made it this far with my studies.

Abstract

Helicobacter pylori is a bacterium with a capacity to evade the host's immune system. Some of these immune evasion mechanisms have been identified, but many remain unknown. The NKG2D receptor is an immunoreceptor implicated in the detection stressed, malignant, infected cells via its ligands. There is growing evidence that host microbiota-mediated modulation of the NKG2D receptor, plays a key role in the genesis and progression of many gastrointestinal disorders. A recent study found no difference between the levels of NKG2D expressed by the lymphocyte populations in normal stomach mucosa and in the stomachs of people suffering from *H.pylori* gastritis. This discovery prompted us to postulate an involvement of soluble NKG2D ligands (MICA and MICB) released by the matrix metalloproteinase ADAM17; a hypothesis that is moreover supported by a previous demonstration of activation of this "shedase" by the protein CagL, a subunit of *H.pylori*'s type 4 secretion system.

In experiments designed to test the above hypothesis, cultured gastric epithelial cell lines were infected with wild type *H.pylori* or a knockout mutant. Quantitative polymerase chain reaction was used to assess subsequent gene expression changes. To determine the actual ligand expression of cells we employed flow cytometric assays. Increased gene expression for both MIC ligands and ADAM17 was observed with MKN28 cells 24 hours after infection. Gene expression of interleukin-15 was also increased starting at 4 hours post-infection. Flow cytometric analyses with 3 different gastric cell lines on the other hand produced highly variable and inconclusive results. Whilst AGS cells infected with the wild type strain expressed lower levels of MIC ligands than those infected with the knockout mutant, an opposite response was observed for the other 2 lines. Altogether, the results paint an unclear picture and further investigations will be necessary to unequivocally prove or disprove our hypothesis.

Zusammenfassung

Helicobacter pylori ist ein Bakterium das Wissenschaftler seit seiner Entdeckung vor Rätsel gestellt hat. Seine Fähigkeit in einer extrem feindseligen Umgebung nicht nur zu überleben, sondern aufzublühen ist erstaunlich. Seine Fähigkeit einen Wirt für langanhaltende Perioden zu infizieren ohne dabei richtig von dem Immunsystem erkannt zu werden, ist genau so rätselhaft und bleibt zum größten Teil bis heute unerklärlich.

So wie andere aktivierende Immunrezeptoren auch, ermöglicht der NKG2D Rezeptor die Erkennung von gestressten, bösartigen und infizierten Zellen mit der Hilfe seiner Liganden. Außerdem zeigen immer mehr Publikationen, dass das NKG2D System eine wichtige Rolle in der Entwicklung und Progression von gastrointestinalen Erkrankungen spielt, da es durch die Mikrobiota des Wirtes moduliert wird. Eine Mitarbeiterin unserer Arbeitsgruppe hat vor kurzem beobachtet, dass im Gegensatz zu gesunden Menschen die Expression des NKG2D Rezeptors in den Mägen von Menschen, welche an *Helicobacter pylori* Gastritis leiden, nicht beeinflusst, oder sogar supprimiert wird. Wir theorisierten, dass diese Herabregulierung durch das Ablösen der NKG2D Liganden MICA und MICB von der Oberfläche der gastrischen Epithelien induziert wird. Dieses Ablösen wird durch die Matrix Metalloproteinase ADAM17 ermöglicht. Es wurde schon gezeigt, dass dieses Enzym durch das Protein CagL, eine Untereinheit des T4SS Sekretionssystem von *Helicobacter pylori*, aktiviert wird. Um unsere Hypothese zu beweisen haben wir Zellkultur-Infektionsexperimente mit gastrischen Zelllinien gemacht. Die zellulären Antworten wurden dann mittels quantitativer Polymerase Kettenreaktion und flowzytometrischer Messungen untersucht. Wir haben festgestellt, dass die Genexpression von MIC Liganden und ADAM17 in der Zelllinie MKN28 nach 24 Stunden alle erhöht waren. Die Genexpression von Interleukin 15 war ebenfalls erhöht, jedoch schon nach 4 Stunden Infektionszeit. Flowzytometrische Analysen wurden mit 3 verschiedenen gastrischen Zelllinien durchgeführt. Die Resultate dieser waren sehr variabel und insgesamt nicht aussagekräftig. AGS Zellen welche mit dem Wildtyp infiziert wurden exprimierten weniger MIC Liganden als Zellen welche mit dem knockout Mutanten infiziert wurden. Wiederum zeigte sich im gleichen Experiment mit anderen Zelllinien eine umgekehrte Reaktion. Insgesamt bietet sich ein unklares Bild des vorgeschlagenen Mechanismus. Weitere Untersuchungen werden notwendig sein um unsere Hypothese zu verifizieren oder sicher zu widerlegen.

Table of Contents

Eidesstattliche Erklärung	ii
Acknowledgments	iii
Abstract	iv
Zusammenfassung	v
Table of Contents	vi
Abbreviations.....	ix
List of figures	xii
List of tables	xii
1 Introduction	1
1.1 The human gastrointestinal tract.....	1
1.1.1 The stomach	1
1.2 Colonisation of the GI tract with microorganisms	5
1.2.1 The stomach microbiota.....	9
1.2.2 <i>Helicobacter pylori</i>	11
1.3 NKG2D receptor.....	14
1.4 Interleukin-15	15
1.5 Aims of this project.....	16
2 Materials and Methods.....	19
2.1 Cell culture	19
2.1.1 Cell lines	19
2.1.2 Cell line cultivation	19
2.1.3 Bacterial cultivation	20
2.1.4 Cellular infection	20
2.1.5 Stimulation with SCFAs	21

2.2	Quantitative polymerase chain reaction (qPCR)	21
2.2.1	RNA extraction.....	21
2.2.2	RNA quantification	21
2.2.3	Reverse transcription (RT)/ cDNA synthesis.....	22
2.2.4	qPCR primers/ primer optimization	22
2.2.5	Actual procedure.....	23
2.3	Flow cytometry.....	23
2.3.1	Cell preparation.....	23
2.3.2	Extracellular staining.....	24
2.3.3	Intracellular staining	24
2.3.4	Actual procedure.....	25
2.3.5	Data correction and analysis	25
3	Results.....	26
3.1	MKN28 Cells infected with wild-type <i>H.pylori</i> show a higher mRNA expression of MICA/B, ADAM17, and IL-15	26
3.2	AGS cells treated with <i>H.pylori</i> WT and CagL knockout exhibit a non-significant increase of extracellular MICA/B	28
3.3	HeLa cells treated with butyrate had a significantly increased MIC ligand expression compared to controls	30
3.4	MKN74	33
3.4.1	WT P12 <i>H.pylori</i> prompts increased MIC ligand expression in MKN74 cells	33
3.4.2	MIC ligand expression of MKN74 cells after 48h stimulation with butyrate is significantly increased vs. controls.....	35
4	Discussion	37
5	References	44

6	Appendix.....	55
6.1	<i>H.pylori</i> agar plates	55
6.1.1	Ingredients for agar solution	55
6.1.2	Vitamin mix for agar <i>H.pylori</i> agar plates	55
6.2	qPCR primers.....	56
6.3	qPCR standard curve protocol	57

Abbreviations

°C	degrees centigrade
µg	microgram
µl	microliter
7-AAD	aminoactinomycin D
AB	antibiotic
Ab	antibody
ACTB	beta-actin
ATP	adenosine triphosphate
ATPase	adenosine triphosphatase
CagA	cytotoxin-associated gene A
cd	coeliac disease
cDNA	complementary deoxyribonucleic acid
CFU	colony forming units
CNS	central nervous system
c-Src	proto-oncogene tyrosine-protein kinase Src
DMEM	Dulbecco's Modified Eagle's medium
DNA	deoxyribonucleic acid
EDTA	ethylenediaminetetraacetic acid
EGFR	epidermal growth factor receptor
ELISA	enzyme-linked immunosorbent assay
FACS	fluorescence-activated cell sorting
FBS	foetal bovine serum
FVD	fixable viability dye
g	gram
GALT	gut-associated lymphoid tissue
GAPDH	glyceraldehyde 3-phosphate dehydrogenase
GI microbiota	gastrointestinal microbiota
GI tract	gastrointestinal tract
h	hours
<i>H.pylori</i>	<i>Helicobacter pylori</i>

H ₂	molecular hydrogen
IBD	inflammatory bowel disease
IEL	intra epithelial lymphocyte
IL-15	Interleukin 15
IL-2	Interleukin 2
L	litre
LPS	lipopolysaccharide
LyG	corpus-dominant lymphocytic gastritis
MALT	mucosal-associated lymphoid tissue
MFI	median fluorescence intensity
mg	milligram
MICA	MHC class I polypeptide related sequence A
MICB	MHC class I polypeptide related sequence B
min	minutes
miRNA	microRNA
ml	millilitre
mM	millimolar
MOI	multiplicity of infection
mRNA	messenger RNA
NK cells	natural killer cells
NKG2D	natural killer group 2 member D
nm	nanometre
NOS2	nitric oxide synthase 2 (inducible nitric oxide synthase)
OMV	outer membrane vesicle
PAI	pathogenicity island
PAMP	pathogen-associated molecular patterns
pH	potential of hydrogen
pmol	picomole
PTP	protein tyrosine phosphatase
RNA	ribonucleic acid
rpm	revolutions per minute

RPMI medium	Roswell Park Memorial Institute medium
RT	reverse transcription
SCFA	short-chain fatty acid
SD	standard deviation
sec	seconds
sMICA	soluble MICA
SN	supernatant
T4SS	type 4 secretion system
TACE	tumour necrosis factor- α -converting enzyme
TK	tyrosine kinase
TNF α	tumour necrosis factor- α
ULBP	cytomegalovirus UL16-binding protein
VacA	vacuolating cytotoxin
WT	wild type

List of figures

Figure 1: Labelled diagram of the human stomach.....	2
Figure 2: Labelled diagram of a gastric gland with gland cells.....	4
Figure 3: Depiction of difference between normal and dysbiotic microbiota.....	6
Figure 4: Diagram explaining the terms microbiota, metagenome, and Microbiome.....	7
Figure 5: Diagram describing the proposed mechanism.....	18
Figure 6: Results of qPCR analysis of infection assay with MKN28.....	27
Figure 7: Results of flow cytometric analysis of infection assay with AGS.....	29
Figure 8: Results of flow cytometric analysis of infection assay with HeLa.....	32
Figure 9: Results of first flow cytometric analysis of infection assay with MKN74.....	34
Figure 10: Results of second flow cytometric analysis of infection assay with MKN74.....	36

List of tables

Table 1: Cell seeding density of various cell lines.....	20
Table 2: Ingredients for agar plates.....	55
Table 3: Ingredients for vitamin mix – first of 2 solutions.....	55-56
Table 4: Ingredients for vitamin mix – second of 2 solutions.....	56
Table 5: qPCR primers used in this thesis.....	56-57

1 Introduction

1.1 The human gastrointestinal tract

The human gastrointestinal tract (GI tract) spans from the oral cavity to the anus. It is vital for human survival as it allows for the digestion and absorption of nutrients from the food we ingest. The human GI tract can be divided into the upper- and lower GI tract; whereby the exact anatomical demarcation between the two is the suspensory muscle of the duodenum. The upper GI tract consists of the oral cavity, pharynx, oesophagus, stomach, and duodenum. The lower GI tract consists of the greater part of the small intestine, as the duodenum is a segment of the small intestine, and the entire colon. The small intestine can be subdivided into duodenum, jejunum, and ileum. Its main function is to absorb nutrients which are released during digestion. The colon consists of the caecum, which has the appendix attached to it, ascending colon, transversal colon, descending colon, sigmoid colon, rectum, and anus. The colon's main function is to reabsorb water which ensures for solid stools.

1.1.1 The stomach

The stomach is a muscular, hollow organ in the upper gastrointestinal tract. It is localised between the oesophagus and small intestine. Anatomically the stomach can be divided into 5 sections: the cardia, fundus, body, antrum, and pylorus. The first section, the cardia, is where the food first arrives when it passes through the lower oesophageal sphincter. The cardia, or cardiac region, is defined as the region following the "z-line" which signifies the epithelial change from stratified squamous to columnar epithelium. The fundus is shaped like a dome sitting on top of the body and is located to the left of the cardiac orifice; gas usually fills it. The stomach's body reaches from the cardiac orifice to the level of the incisura angularis which represents a constant notch in the lower segment of the lesser curvature. It serves as a reservoir for incoming food and can expand to a great extent. The antrum is a segment reaching from the incisura angularis to the pylorus. Finally, the pylorus is the last part of the stomach as it serves as a valve separating the stomach from the duodenum. Its thick muscular wall is called the pyloric sphincter which enables it to control the emptying of gastric contents and thus limit the premature passing of large food pieces and undigested material into

the small intestine (Fig. 1). Histologically the stomach can be divided into 3 regions (cardia, fundus, pylorus) depending on the types of glands which can be found there.

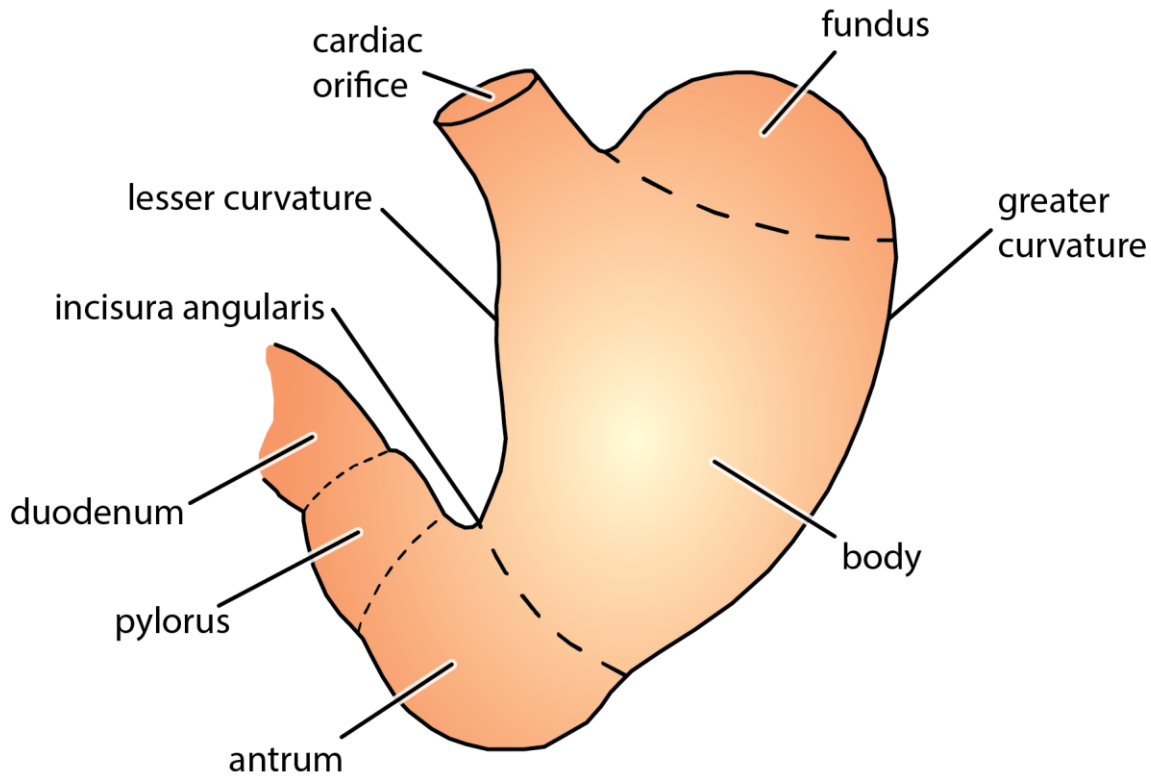


Figure 1 Simplified depiction of the human stomach divided into its anatomical sections.

From a functional standpoint, the stomach fulfils some functions which are essential for adequate digestion. Food which is chewed up in the oral cavity is transported through the oesophagus as a food bolus. It enters the stomach through the lower oesophageal sphincter. Specialised exocrine cells found in the lining of the stomach mucosa then begin secreting various substances which aid in the digestive process. Surface mucous cells secrete mucus into the lumen of the stomach. These can be found lining the entire surface of the stomach. A similar function is carried out by mucous neck cells. However, these gland cells are located in the upper section of the gastric pits. These represent indentations in the gastric mucosa which denote the entrance to the tubular gastric glands. Mucus is rich in bicarbonate ions and thus creates a protective barrier against

enzymes and acid. There are two important types of tubular glands: oxyntic glands (or gastric glands) and pyloric glands. The oxyntic glands include two additional types of exocrine cells: chief cells and parietal cells. Chief cells produce the two digestive enzymes pepsinogen and gastric lipase. Parietal cells secrete intrinsic factor, a glycoprotein which binds vitamin B12, and hydrochloric acid. Gastric juice, composed of the various gastric gland secretions, has a pH of 1 - 3.5. The pH of the gastric juice varies depending on the concentration of hydrochloric acid. Finally, pyloric glands include the so-called G cells. These are cells located deep in the gastric pits that secrete the peptide hormone gastrin. As these are endocrine cells, their secretions are not released into the lumen, but rather into the bloodstream. Gastrin is a hormone which stimulates the secretion of hydrochloric acid by parietal cells and aids gastric motility (Fig. 2).

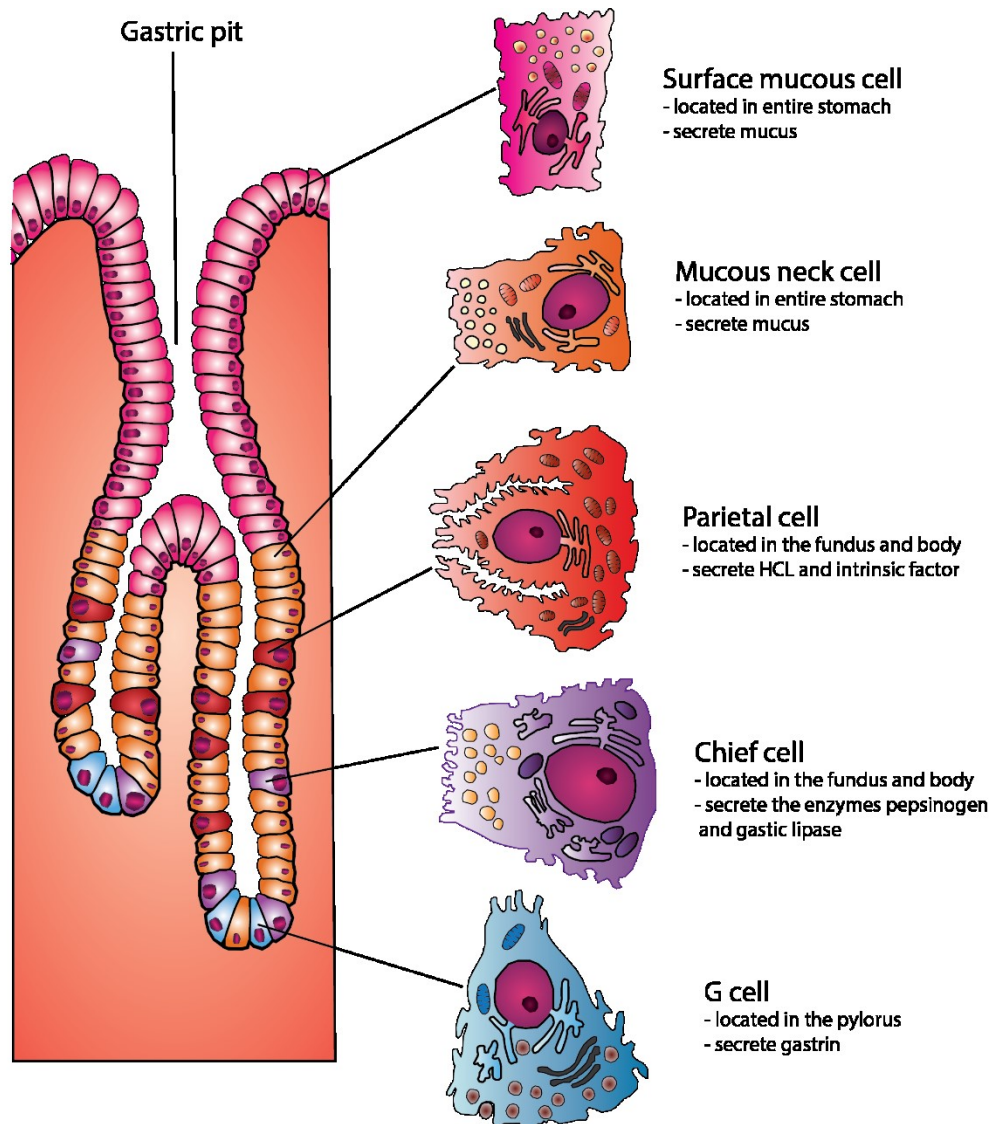


Figure 2: Simplified depiction of a gastric pit with the various gastric gland cells.

The low pH of the gastric juice plays a key role in the digestion of protein. On the one hand, the highly acidic environment leads to the denaturation of proteins exposing their peptide bonds. This makes them more susceptible to enzymatic cleavage by proteases. On the other hand, the low pH leads to the conversion of pepsinogen into the active proteolytic enzyme pepsin. The gastric juice's pH represents the optimum pH for pepsin to function as an active proteolytic enzyme (1). Furthermore, it has been shown that mice with a mutation in a gastric H^+/K^+ -ATPase (proton pump) gene resulting in hypochlorhydria (reduced hydrochloric acid secretion in the stomach) showed

increased susceptibility to infection with specific bacterial pathogens (2). It was also shown previously that, regardless of cause, hypochlorhydria is associated with a greater risk of infection (3,4). Mounting evidence finds that the widely prescribed drugs known as proton pump inhibitors, which essentially cause hypochlorhydria, are strongly associated with a greater risk of infection with the intestinal pathogen *Clostridium difficile* (5–8). This suggests that the stomach's harsh acidic environment plays a vital role in pathogen resistance.

1.2 Colonisation of the GI tract with microorganisms

Like many regions of the body, the GI tract is colonised by various microorganisms which are referred to as the gastrointestinal microbiota. The term flora has become outdated as it does not sufficiently account for the many non-bacterial organisms such as archaea, viruses, and fungi (9). There are many technical terms used in this field. To avoid confusion, the most common terms will be visualised and briefly explained and in figure 3 and 4 as described in a review paper by Whiteside et al. (10):

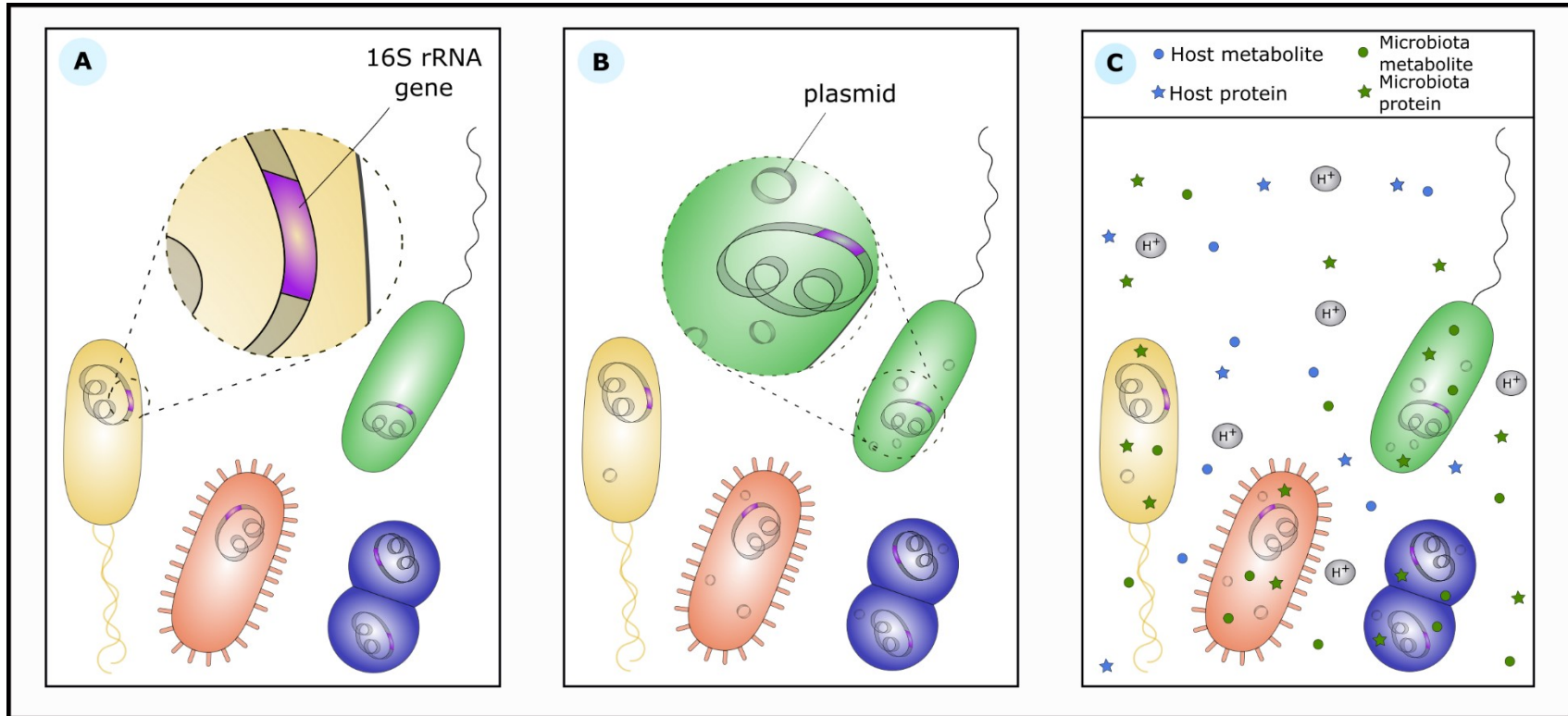


Figure 3: (A) **Microbiota**: the different microorganisms in a specific region/environment. These are commonly identified using 16s rRNA surveys which allows for taxonomic identification. (B) **Metagenome**: the genes and genomes of the corresponding microbiota. This also includes plasmids which can elucidate intra-species variances. (C) **Microbiome**: refers to the different genes and genomes of the microorganisms which make up the microbiota, as well as the products of the microbiota and the host environment (i.e. microbiota and host metabolites and proteins). (Figure adapted from Whiteside et al., 2015)³

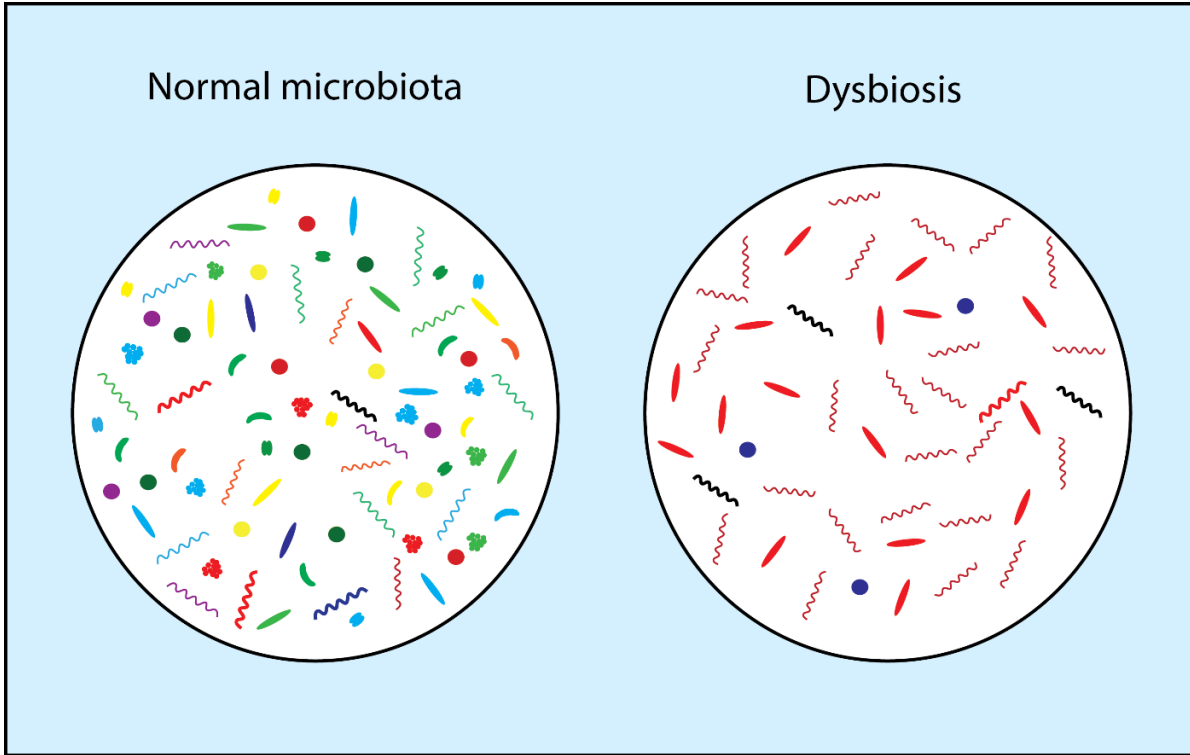


Figure 4: **Dysbiosis**: a term used to describe an imbalance in the composition of the microbiota. It is commonly used to describe a state of reduced diversity, meaning that fewer different bacterial strains are present. Whereby the bacteria which remain “overgrow” the ecological niche and can become detrimental for the host.

Environmental factors shape the microbiota of a specific body region. These include factors such as abundance of specific nutrients, presence of oxygen, temperature, pH, and moisture. For example, the skin offers a variety of different niches with regions offering a broad range of pH, temperature, moisture, and sebum. Each of these niches may be associated with their own unique microbiota (11). Similarly, the GI microbiota offers a variety of different environmental niches resulting in region specific microbial compositions. The oral cavity offers a rapidly changing environment in which nutrients may be at times highly abundant and at others relatively scarce. Influx of foods and liquids means that resident microbes constantly risk being swept away. For this reason, some autochthonous bacterial species rely on forming biofilms on teeth (plaque) in which they may seek refuge and establish a relatively stable environmental niche (12).

The gut represents a somewhat different niche as its contents pass through it more slowly and it offers a great abundance in nutrients vital to certain bacteria. It therefore comes as no surprise that the gut accommodates the largest number of bacteria and the greatest number of bacterial species compared to other body regions (9). However, it is becoming increasingly clear that the environmental niche of the gut may not be as conserved as formerly assumed. Microbiota analyses done with 16s rRNA gene sequencing show that the gut microbiota varies greatly depending on which food is being consumed. It has been shown that a low-fibre diet can lead to veritable extinctions in a number of resident bacterial strains (13). These changes to the bacterial composition can in fact change as rapidly as between meals, whereby certain foods would promote the growth of some strains and inhibit the growth of others (14). Factors such as host genetics as well as disease states have also been shown to contribute towards altering the microbiota. However, with the term dysbiosis being used ever more frequently, the question remains: what is a “normal” microbiota?

Especially in the last decade, the body’s microbiome has become a major topic in popular media. This is partly owing to the fact that there are an increasing number of reports which indicate that the microbiome has a substantial impact on our health and well-being. Alterations in the composition of the gut microbiota have been linked to

diseases such as cardiovascular disease, inflammatory bowel disease, allergies, and diabetes (9,15). There have also been increasing reports showing that the gut microbiome can communicate with the central nervous system (CNS) – the so-called gut-brain axis. In this way, the gut microbiome can influence brain function, behaviour, and even brain development (16–19). While it is not yet clear how exactly this gut-CNS communication takes place, it is intriguing to think that a single meal may cause disturbance in the gut's microbial composition. A disturbance which could potentially influence a person's mood.

Furthermore, a growing body of evidence see the body's various microbiomes implicated in the development and regulation of the immune system. A body region which has been studied closely in this regard is the GI tract; specifically, the gut. This region has been an object of such interest because it is by far the most densely populated by microorganisms (20,21). Moreover, the gut-associated lymphoid tissue (GALT) is the largest constituent of the mucosa-associated lymphoid tissue (MALT) and is thus inhabited by almost 70% of the entire immune system (22). A reciprocal relationship exists between the microbiota and the immune system. The immune system utilises IgA antibodies, miRNA, and other immune responses to shape the microbial composition (23,24). Whereby the microbiota interacts with the host by employing a variety of different substances such as metabolites like short-chain fatty acids (SCFAs), microbe derived nucleic acids, quorum sensing (QS) signals, and outer membrane vesicles (OMVs)(25,26). It is also important to note that bacterial communities shape and regulate themselves through a number of different mechanisms (27).

1.2.1 The stomach microbiota

As mentioned above, the stomach represents a unique environment for microorganisms as the gastric juice secreted by the various gastric glands is highly acidic. In fact, up until the discovery of *Helicobacter pylori* (*H.pylori*) in 1982 by Marshall and Warren, the stomach was considered sterile since it represents such a harsh environment (28). More recent studies have now shown that *H.pylori* is not the only bacterium that can be found in the stomach. However, depending on the sample site,

either gastric fluid or the gastric mucosa, the microbial compositions vary distinctly. A study by Bik et al. found that gastric fluid is mainly inhabited by Firmicutes, Bacteroidetes, and Actinobacteria. The Firmicutes were mainly of the genus *Streptococcus* and the Bacteroidetes mainly of the genus *Prevotella* (29). These bacteria represent common representatives of the oral microbiota (12). It is therefore reasonable to assume that these do not colonise the stomach permanently, but may rather constitute a transient microbiota which rapidly varies depending on swallowed microorganisms (30). The gastric mucosa was shown to be colonised mainly by Firmicutes and Proteobacteria (including *H.pylori*). In patients infected with *H.pylori*, Proteobacteria was by far the predominant phylum constituting around 96% of all bacteria. Intriguingly, despite this seeming Proteobacteria “overgrowth” in *H.pylori* positive subjects, when *H.pylori* sequences were not included in the analysis, phylotype evenness and diversity were higher than in *H.pylori*-negative subjects (29). Thus, one could argue that *H.pylori* counteracts dysbiosis, as dysbiosis represents a state of reduced bacterial variation.

It is also a common misconception that *H.pylori* constitutes the sole pathogen capable of infecting and causing disease in the stomach. For example, patients with corpus-dominant lymphocytic gastritis (LgG) were first suspected of suffering from *H.pylori* induced gastritis. Even once LyG had been identified as a distinct disease, *H.pylori* was suspected of playing a role in its aetiology. However, this has since been disproven (31). It has also been seen to correlate with coeliac disease (cd) as a study in 1999 found that 38% of 103 LyG patients also suffered from cd (32). However, a definitive mechanism connecting cd and LyG has not yet been found. Interestingly, despite the fact that *H.pylori* could not be found in the stomachs of LyG patients, antibiotic (AB) *H.pylori* eradication therapy had a positive effect on the disease development; suggestive of bacterial involvement. In fact, it has now been shown that *Propionibacterium acnes* may be the causative pathogen as it was found in comparative microbiota analyses of samples taken from LyG patients (33). In general, the stomach microbiota is still poorly understood compared to the microbiota of other body regions. Further studies will be needed to fully understand its development and physiological importance.

1.2.2 *Helicobacter pylori*

H.pylori is a gram-negative bacterium belonging to the Proteobacteria phylum. It is helix-shaped and is roughly 3 µm long and 0.5 µm thick. It forms biofilms (34) and under harsh conditions can convert from a spiral to a coccoid form, from which it can no longer be cultured. However, it is unclear if it is still viable in this form (35). *H.pylori* possess a unipolar bundle of 2 to 6 sheathed flagella which are composed of two copolymerized flagellins, FlaA (36) and FlaB (37). The bacterium's many flagella allow it to move freely in its ecological niche, the mucous layer of the gastric epithelium(38). These have been shown to be essential for both stable colonisation of the human gastric mucosa (39) as well as the bacterium's pathogenicity (40,41). It is a microaerophilic bacterium which means that while it needs oxygen to survive, it requires environments with lower levels of oxygen than are present in our atmosphere (2-10% O₂ vs <21% O₂) (42). As it possesses a hydrogenase, it can produce energy by oxidizing the molecular hydrogen (H₂) produced by other bacteria (43). Furthermore, it produces an enzyme known as urease which catalyses the hydrolysis of urea into ammonia and carbon dioxide. While urease is produced by a number of bacteria and fungi, it has become primarily associated with *H.pylori* as it is implicated in the pathogenesis of diseases mediated by the bacterium. These include peptic ulcers and hepatic encephalopathy (44,45). Urease has also become an important diagnostic marker: The so-called rapid urease test exploits the pH shift which ensues from the catalytic reaction mediated by the enzyme and so allows for quick detection of *H.pylori* in, for example, a stomach biopsy.

H.pylori is a bacterium which has become relatively well known as the pathogen responsible for causing infectious gastritis and peptic ulcers. Of late, it has additionally become notorious as it was the first bacterial species to be recognised as a carcinogen (46). Its presence has been linked to the development of both gastric adenocarcinoma and gastric MALT lymphoma (47,48). It has therefore become common practice amongst physicians to pursue a swift eradication of the bacterium when a *H.pylori* infected individual has been identified. However, at the same time a steady decline of *H.pylori* infection rates has been observed in developed countries. It has been proposed that this inverse correlation of infection rates with improving sanitary conditions may be linked to the increasing rates of allergic and immunological diseases.

For example, a meta-analysis involving 28,283 patients found a significantly lower rate of *H.pylori* infections in patients suffering from asthma (49) and other studies have found similar results (50–52). Furthermore, studies have found that being infected with *H.pylori* as a child may be protective of other immunologically mediated diseases such as food allergies and celiac disease (53,54). However, it is not yet clear how these effects are mediated and there have been contradictory studies in which the results show no such correlations (55–58).

H.pylori possesses two secreted toxins: vacuolating cytotoxin (VacA) and cytotoxin-associated gene A (CagA). These toxins are employed to manipulate host tissues, thus promoting the bacterium's own persistence. VacA is a pore-forming toxin which has been shown to disrupt epithelial cell polarity and tight junctions, promote apoptosis in epithelial cells, and inhibit T-cell proliferation as well as T-cell associated effector functions. The VacA gene has been seen to be carried by all *H.pylori* strains and differing expression of the gene is linked to varying pathogenicity of the respective strains (59). CagA, a further important secreted toxin, is considered to be an oncoprotein as CagA expressing strains are associated with an increased risk of gastric cancer. *H.pylori* employs a type IV secretion system (T4SS) to “inject” CagA into the host cell. Upon entering, CagA localises to the plasma membrane and is phosphorylated by a host cell membrane-associated tyrosine kinase (TK). This then leads to the allosteric activation of protein tyrosine phosphatase (PTP) SHP2. This may contribute to the oncogenicity of the toxin as it has been shown that mutations in the gene that encodes for human SHP2 lead to haematological malignancies and contribute towards the pathogenesis of childhood leukaemia (60). Particularly pathogenic strains of *H.pylori* have been shown to additionally activate the epidermal growth factor receptor which is associated with altered signal transduction and gene expression in host epithelial cells and may also contribute towards oncogenicity. CagA is encoded on the cag pathogenicity island (PAI) which also encodes for the cag T4SS. The Cag T4SS plays an essential role during infection and determines its severity as it is necessary for CagA translocation (61). It constitutes a needle-like pilus which is comprised of numerous Cag PAI encoded proteins; some of which are essential for

pilus formation (62). Furthermore, T4SS and the proteins it is comprised of, have been seen to directly interact with host cells via integrin molecules (63).

In this study we have concentrated on the protein CagL, as it has been shown that CagL deficient mutants are unable to form the T4SS pilus (64). CagL has been seen to specifically bind to the integrins $\alpha_5\beta_1$ and $\alpha_V\beta_5$ (63). This has been seen to be implicated in a variety of host cell interactions and signal transductions. For example, CagL binding to the integrin $\alpha_V\beta_5$ has been shown to lead to an upregulation of gastrin expression which is mediated via an integrin linked kinase (ILK) signalling complex (65). The binding to of CagL to $\alpha_5\beta_1$ has been shown to trigger cell spreading, focal adhesion formation, and the activation of several tyrosine kinases. These include the epidermal growth factor receptor (EGFR) and EGFR family member Her3/ErbB3 (66) both of which have been shown to be implicated in the development of a number of cancers(67) and inflammatory diseases(68). It also activated the non-receptor tyrosine kinases focal adhesion kinase (FAK) and Proto-oncogene tyrosine-protein kinase Src (c-Src); both of which have been shown to be associated with various cancers (69,70). Furthermore, the binding of CagL to $\alpha_5\beta_1$ was shown to lead to the dissociation of the enzyme ADAM17, also called tumour necrosis factor- α -converting enzyme (TACE). As one of its names already suggests, the metalloprotease ADAM17 plays a key role in the processing of the pro-inflammatory cytokine tumour necrosis factor α (TNF α)(71). It is furthermore understood to be involved in the cleavage of a variety of membrane-bound proteins; a process known as shedding. This involves the cleavage and release of the soluble ectodomain from membrane-bound pro-proteins. ADAM17 expression has been seen to negatively correlate with outcomes of various cancers. This is due to chemo- and radiotherapy induced activation of ADAM17 which enables the shedding and activation of growth factor-mediated pro-survival response (72). Moreover, the shedding of immunoreceptor ligands by ADAM17 has been shown to be a key immune escape mechanism exploited by cancer (73).

H.pylori is the perfect example of a bacterium completely adapting to its human host. It has been infecting humans for at least 60 thousand years. This has allowed it to co-evolve with its host and continuously adapt throughout our joint evolution (74). In fact,

H.pylori has become so accustomed to its human host that it does not infect the stomach of other animals. This made creating a mouse model to study a persistent infection in more detail a serious challenge. To account for this, rodent-adapted strains were developed to study the bacterium in vivo (75). Over the years the bacterium has developed a myriad of different mechanisms to evade the host immune system. To name a few: *H.pylori* possesses pathogen-associated molecular patterns (PAMPs) which have evolved to evade detections by pro-inflammatory Toll-like receptors (TLRs)(76,77). It has been shown that *H.pylori* secretes OMVs which can indirectly inhibit T-cell responses by inducing cyclooxygenase-2 (COX-2) activity in monocytes (78). Reports have indicated that *H.pylori* employs macrophage arginase 2 to limit nitric oxide (NO) production by macrophages, neutrophils, and epithelial cells by depleting intra- and extracellular L-arginine; a substrate necessary for NO production by nitric oxide synthase 2 (NOS2)(79).

1.3 NKG2D receptor

The NKG2D receptor is an activating immunoreceptor found on natural killer (NK) cells, T cells, and macrophages. NKG2D has been seen to be important for NK cell and T cell mediated defence against viruses and tumours. Reports have shown it to play a role in autoimmune diseases, allogenic transplantation, and xenotransplantation (80). NKG2D ligands in humans can be grouped into two families; the MHC class I polypeptide related sequence protein family of which there are two variants: A (MICA) and B (MICB) and the cytomegalovirus UL16-binding protein (ULBP) family. Ligands originating from different families are highly polymorphic and show few similarities regarding sequence or domain structure (81). It is therefore compelling that all these ligands can bind to NKG2D with high affinity. The diversity of NKG2D-ligands may facilitate the recognition of rapidly evolving pathogens or cancers (82).

In general, NKG2D-ligands have been regarded as ligands which allow the recognition of “stressed” or “damaged” cells by the immune system. However, recent work has reported NKG2D ligand expression on healthy cells. The first “healthy” cells reported to show such an expression pattern were gut epithelial cells. As epithelial cell lines exhibit an up-regulation of NKG2D-ligands when exposed to bacteria (83), it can be

assumed that the NKG2D-ligand expression is responsive to the microbiota. Interestingly a low constitutive NKG2D-ligand expression pattern did not lead to immune responses directed against the gut epithelium. However, in autoimmune conditions such as Crohn's disease and celiac disease, intestinal epithelial cells are targeted and killed by NKG2D⁺ intra epithelial lymphocytes (IELs)(84,85). Thus, it can be assumed that gut epithelial cells show a low constitutive expression of NKG2D ligands under physiological conditions. Yet an increased expression can be regarded as a breakdown of immune tolerance. Recent studies have shown that a number of other tissues express NKG2D-ligands physiologically. These include haematopoietic cells, embryonic tissues, airway epithelial cells, neurons, hepatic cells, and skin (86). Further research will be necessary to fully elucidate the complex functional roles of NKG2D in diseased and healthy tissues.

1.4 Interleukin-15

Interleukin-15 (IL-15) is a cytokine sharing structural similarity with interleukin-2 (IL-2). IL-15 signalling is mediated via a receptor complex consisting of IL-2/IL-15 receptor beta chain and the common gamma chain. Unlike IL-2, it is produced and secreted by monocytic phagocytes, dendritic cells, and other cell types such as keratinocytes, fibroblasts, and nerve cells (87). Its main function is mediating the proliferation, activation, and differentiation of NK cells. However, its effects vary depending on the target cell. For example, IL-15 inhibits apoptosis in various other immune cells, such as $\gamma\delta$ T cells, mast cells, and intraepithelial lymphocytes. It has been shown to increase the expression of co-stimulatory molecules and INF-gamma-release and it has been reported to play a role in the maintenance of memory T cells (88). Thus, IL-15 is regarded as a key player of inflammatory processes and acts on both the innate, as well as adaptive immune system. It has been implicated in the pathogenesis of various gastrointestinal diseases including inflammatory bowel disease (IBD), celiac disease, and colorectal cancer (88). We decided to include it in our investigation because of its important role regarding NK-cells and its known involvement in the development of various gastrointestinal diseases.

1.5 Aims of this project

It is becoming increasingly clear that the mechanisms which *H.pylori* employs to avoid detection by the host immune system are highly diverse. We have above described some of the mechanisms *H.pylori* employs to escape detection by the host immune system. Up till now only little is known of the role which the NKG2D receptor plays in the long-term infection or rather colonisation of the stomach mucosa with *H.pylori*. However, in her PhD thesis, A. Montalban-Arques was able to show that the expression of the NKG2D receptor in the gastric mucosa of *H.pylori* infected individuals remained equal or even below that of healthy individuals (33). This would indicate that *H.pylori* is able to inhibit NKG2D expression in order to escape detection by the immune system. To elucidate the mechanism behind this response we began by studying associated literature. A study reported that the presence of tumour derived soluble MICA (sMICA) led to the downregulation of the NKG2D receptor in cancer patients (89). Furthermore, we found that MICA has been shown to be shed by ADAM proteases; specifically ADAM10 and ADAM17 (90). An in-depth literary review regarding these metalloproteinases revealed that the expression of ADAM17 is regarded as a valuable prognostic marker regarding human gastric cancer (91); a disease which is also closely linked to *H.pylori*. It was also shown that, *H.pylori* can directly activate ADAM17 via its T4SS subunit CagL (92). In sum, these reports point towards a mechanism in which *H.pylori* activates ADAM17 via the CagL protein. This in turn would lead to the shedding of MICA ligands. These sMICA ligands could bind to NKG2D receptors on immune cells, resulting in their downregulation (Fig. 4). Proving this mechanism may allow the development of novel treatments for *H.pylori* gastritis. Targeted therapies could block specific steps in the mechanism potentially enabling the host immune system to better recognise and clear the bacteria by itself. It would therefore represent a targeted alternative to antibiotics; pharmaceuticals which can have severe adverse effects and are simultaneously a dwindling commodity. However, this mechanism may be exploited in a reverse manner: It is possible that this immune-dampening effect could be used in the therapy of allergies, autoimmune diseases, other immunological diseases, and cancer.

To prove that the proposed mechanism does indeed apply, we decided to employ cell culture experiments with various established gastric cell lines. We infected these cells with both a WT- and CagL knock-out *H.pylori* strain. We then assessed for differences in the messenger RNA (mRNA) expression of MIC ligands, IL-15, and ADAM17 using quantitative polymerase chain reaction (qPCR). We then assessed both the extra- as well as intracellular expression of MIC ligands separately using flow cytometry. Due to technical difficulties, we were unable to measure the intracellular expression of one cell line and therefore opted to measure the overall expression (intracellular + extracellular

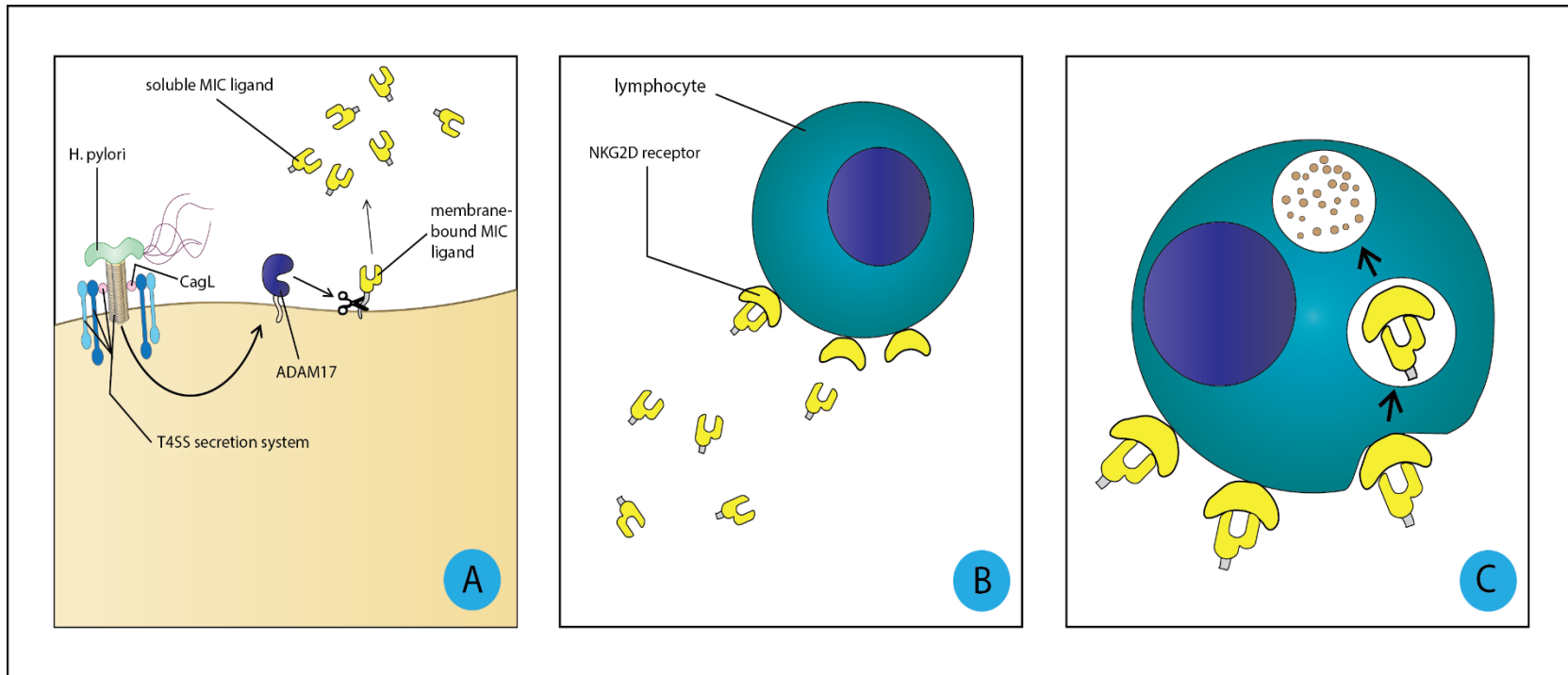


Figure 5 Visualization of the proposed mechanism. (A) *H.pylori* induces the activation of the matrix metalloproteinase ADAM17 via the T4SS secretion system protein component CagL. This in turn cleaves membrane-bound MIC ligands resulting in the liberation of soluble MIC ligands. (B) Soluble MIC ligands bind to lymphocytes expressing the NKG2D receptor (e.g. NK-cells, $\gamma\delta$ T cells). (C) Bound soluble MIC ligands are internalised and degraded in lysosomes. Thus, the surface expression of the NKG2D receptor is down-regulated(c).

2 Materials and Methods

2.1 Cell culture

2.1.1 Cell lines

AGS cells (human gastric adenocarcinoma cell line) were purchased from CLS Cell Lines Service GmbH (Eppelheim, Germany). MKN28 cells (human gastric, moderately differentiated, tubular adenocarcinoma cell line) and MKN74 (human gastric, moderately differentiated, tubular adenocarcinoma cell line) were kindly provided by Dr. S. Wessler(93). The HeLa (human cervical carcinoma cell line) cell line was obtained from the Center of Medical Research (ZMF), Medical University of Graz, Austria

2.1.2 Cell line cultivation

AGS, MKN28, MKN74 were cultivated in Roswell Park Memorial Institute medium (RPMI) 1640 medium (Gibco) supplemented with 10% foetal bovine serum (FBS) (Gibco) and 2 mM L-glutamine (Sigma-Aldrich). HeLa cells were cultivated in Dulbecco's Modified Eagle's medium (DMEM) (Gibco) with 10% FBS (Gibco). Cells grew incubated in a water-saturated atmosphere with 5% CO₂ at 37°C. Cell viability was examined by a CASY® cell counter. For passaging; the cells were first washed with phosphate buffered saline (PBS) (Gibco). Cells were then dissociated by incubating with trypsin-EDTA (Sigma-Aldrich) for 5 min. at 37°C. Trypsin activity was inhibited by adding medium with FBS. Cell counting as well as viability assessment was done using a CASY® cell counter (OMNI Life Science). Cell stimulation or infection was done in 6-well plates 48 h after seeding. The final volume per well was 3 ml of medium-cell suspension. Seeding densities were chosen to ensure for 80% confluence at the time of infection. As cell size and replication rates varied between cell lines different seeding densities were chosen for each cell line. Seeding densities for each cell line can be found in table 1.

Cell line	Cells per well
AGS	1.5×10^5
MKN28	3.8×10^5
MKN74	3×10^4
HeLa	1.5×10^5

Table 1: Seeding density per 6-well plate well of the various cell lines used

2.1.3 Bacterial cultivation

Wild type (WT) and CagL knockout (Δ CagL) P12 *H.pylori* strains were kindly provided by Dr. S. Wessler (93). Bacteria were grown on self-made agar plates. The ingredients used can be found in the appendix under 6.1. For cultivation of bacteria before infection assays, bacteria were taken from frozen stocks at -80°C and sterile cotton swabs were used to retrieve them from the stocks. The bacteria were then spread densely onto prepared agar plates. As *H.pylori* is a microaerophilic bacterium, all the plates were then transferred into anaerobic jars together with sufficient microaerobic generators (Biomérieux) to ensure for microaerobic conditions during incubation.

2.1.4 Cellular infection

Infection assays with *H.pylori* strains were carried out with bacteria suspended in the cell lines' respective medium as stated above. However, lower concentrations of FBS were used (2.5%) as bacterial growth inhibition could be observed when using higher concentrations of FBS. On the day of infection, the cell count of one 6-well plate well was ascertained using a CASY cell counter. As *H.pylori* strains have been seen to grow poorly in liquid culture, they were cultured on agar plates. The colonies were harvested with sterile cotton swabs and then dispersed in 5ml of medium. Subsequently, the OD600 was used in order to ascertain the colony forming units (CFU) of the bacterial suspension, which was additionally measured retrospectively by plating. The CFU of this stock bacterial suspension and the cell count per well were used to calculate and prepare a dilution targeting a multiplicity of infection (MOI) of 1:50. Cells were infected for 24 and 48 h and the CFU/ml were monitored at each time point. This was done by transferring dilutions of homogenised cells and supernatant to agar plates. These agar

plates were incubated at 37°C in microaerophilic conditions until bacterial colonies were visible and countable.

2.1.5 Stimulation with SCFAs

Additionally, cell lines were stimulated with the SCFA butyrate. This was done by preparing medium with 5 mM of butyric acid (Sigma Aldrich). Three ml of this medium was then added to the cells in each 6-well plate well. Cells were harvested and analysed at the same timepoints as the *H.pylori* infected cells.

2.2 Quantitative polymerase chain reaction (qPCR)

2.2.1 RNA extraction

RNA extraction was done using a NucleoSpin® RNA extraction kit (Machery-Nagel). RNA extraction was then performed according to manufacturer's instructions. In brief, the adherent cells were first washed with 1 ml of PBS. 500 µl of trypsin was added to facilitate cellular detachment. After 5 minutes of incubation at 37°C the trypsin was deactivated by adding 500 µl of medium. The cell suspension was collected and centrifuged at 300 x g for 5 min. Cells were then lysed by adding the lysis buffer included in the kit. As RNA extraction was not possible on the same day, samples were subsequently frozen at -80°C. On the day of RNA extraction samples were retrieved from -80°C storage and were thawed on ice. RNA was extracted according to the protocol "RNA purification from cultured cells and tissue" included in the kit. After extraction and purification, the RNA concentration of the samples was measured as described in 2.2.2. They were thereupon transferred to -80°C for long-term storage.

2.2.2 RNA quantification

RNA concentration of samples was measured using the NanoDrop™ 2000c (Thermo Fisher Scientific). Samples were kept on ice at all times to prevent RNA degradation. The instrument was set to the setting "Nucleic acid". Thereafter 5 µl of ultra-pure deionized water was loaded onto the measuring pedestal as a blank. After defining the blank the sampling arm was raised and both the upper as well as the lower pedestal were wiped clean with a lint-free laboratory wipe. Sample RNA concentration was then measured by loading 1.5 µl of each sample onto the measuring pedestal. After each sample measurement both the upper and lower pedestal were wiped. After the

measurement of the final sample 5 µl of ultra-pure deionized water was loaded onto the pedestal as to clean the sensor and to evaluate whether a difference between the blank could be detected; as this would indicate potential false readings. Sample purity was evaluated by means of the purity ratios 260/280 and 260/230 nm wavelengths.

2.2.3 Reverse transcription (RT)/ cDNA synthesis

Reverse transcription was done using the RNA samples which were reverse transcribed on the day following their quantification. Samples were stored at -20°C overnight and were kept on ice at all times when thawed. The target concentration of the cDNA was 1 µg RNA in 20 µl. The RNA concentration of the samples was used to calculate how much of the sample was needed as to achieve 1 µg of RNA in 10 µl. The remaining volume was substituted with RNAase-free water (Qiagen). The High Capacity cDNA Reverse Transcription kit (Applied Biosystems) was used and the standard protocol was followed. To ensure for no RNA degradation a RNAase inhibitor (Applied Biosystems) was added at the standard concentration according to the product protocol. cDNA synthesis was done in 200 µl 8-strip tubes in a 2720 Thermal Cycler (Applied Biosystems). The following protocol was used:

1. 10 min, 28°C
2. 120 min, 37°C
3. 5 min, 85°C
4. hold, 4°C

Once the protocol was finished 80 µl of ultra-pure deionised water was added to each sample and they were then transferred to -20°C for storage.

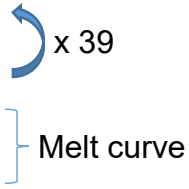
2.2.4 qPCR primers/ primer optimization

Primer efficiency was evaluated by means of standard curves. This was done by running the standard qPCR thermocycler protocol and plating various concentrations of cDNA. The cDNA concentrations employed can be found in the appendix under 6.3. The software *MultiD GenEx* was used to correct results for varying primer efficiency and normalise them to the reference genes beta-actin (ACTB) and Glyceraldehyde 3-phosphate dehydrogenase (GAPDH). Furthermore, a heat gradient was used to assess the ideal primer annealing temperature. Finally, to assess for specific and

consistent amplification products, melting curves were analysed and the amplified PCR-fragments retrieved from the qPCR plate were analysed on agarose gels.

2.2.5 Actual procedure

Quantitative PCR was performed with a CFX96 and CFX384 qPCR thermocycler (BioRad) using SYBR® Green PCR Master Mix (Applied Biosystems). A standard protocol for SYBR® Green was used which also included a melt curve. The following protocol was used:

1. 10 min, 95°C
 2. 15 sec, 97°C
 3. 1 min, 60°C
 4. 15 sec, 60°C
 5. 95°C
- 

The oligonucleotide primers used can be found in the appendix **6.2**. Each reaction had a volume of 10µl. The reaction volume was comprised of 4µl of a 5ng/µl cDNA solution; whereby the cDNA was solved in ultra-pure deionised water. The remaining 6µl were a master mix containing 5µl of SYBR master mix and 0.5µl of both forward and reverse primers at a concentration of 0.25 pmol/µl.

For each mRNA target, gene expression was normalized by using ACTB and GAPDH as house-keeping genes and primer efficiency was also accounted for. Each sample was measured in technical triplicates and the arithmetic mean was used to combine these.

2.3 Flow cytometry

2.3.1 Cell preparation

Cells were cultivated and infected as described in 2.1.2-5. Cells were harvested after 24 and 48 h using either trypsin or Accutase® (Thermo Fisher Scientific). As we found that trypsin cleaves all membrane bound MICA/B ligands, we used this method of dissociation for analysis of intracellular MICA/B ligands. Accutase® was not found to have this effect if incubation at 37°C did not surpass 5 min. It was therefore chosen for assessing the cells' extracellular MICA/B ligand expression. After harvesting, cells were

centrifuged for 3 min at 500 x g. The supernatant was discarded and the cells were resuspended in 200 µl of eBioscience™ Flow Cytometry staining buffer (Thermo Fisher Scientific). 100 µl of each cell suspension was transferred to FACS tubes and stored at 4°C before staining.

2.3.2 Extracellular staining

For extracellular staining, 5µl (0.125 µg) of Alexa Fluor 647 anti-human MICA/B Antibody (Ab) (Biolegend) was added to all cells which were harvested using Accutase® and they subsequently were vortexed gently. The cells were then incubated with the Ab for 30 min at 4°C, protected from light. After incubation, the cells were washed by adding 0.9 ml of staining buffer to the cells and then centrifuging them for 5 min at 500 x g. The supernatant was discarded and the cells were washed again using the same procedure. After again discarding the supernatant the cells were resuspended in 200 µl of staining buffer. To assess cell viability the cells were finally incubated at room temperature (RT) for 5 min with 5 µl of eBioscience™ 7-Aminoactinomycin D (7-AAD) viability staining solution (Thermo Fisher Scientific).

2.3.3 Intracellular staining

Cells were first washed twice with PBS as was described in 2.3.2. Cells were then resuspended in 500 µl of PBS and 0.5 µl of eBioscience™ fixable viability dye eFluor 506 (FVD) (Thermo Fisher Scientific) was added to the cells. The suspension was then gently vortexed and incubated for 30 min at 4°C, protected from light. Cells were then again washed twice, this time with 0.9 ml of staining buffer. After discarding the supernatant, the cells were resuspended in 100µl of eBioscience™ fixation buffer (Thermo Fisher Scientific) and incubated for 20-60 min at RT protected from light. After incubation, 0.9 ml of eBioscience™ permeabilization buffer (Thermo Fisher Scientific) was added to the cells whereupon they were centrifuged for 5 min at 500 x g and the supernatant was discarded. This was done twice and thereupon the cells were resuspended in 100 µl of permeabilization buffer. 5 µl (0.123 µg) of MICA/B Ab was added to each cell suspension and they were immediately vortexed gently. Cells were incubated at RT for 30 min, protected from light. After incubation cells were washed

twice with 0.9 ml of permeabilization buffer and finally resuspended in 200µl of staining buffer.

2.3.4 Actual procedure

A CytoFLEX S flow cytometer (Beckman Coulter) was used to analyse the samples. Measurement was done according to the device manufacturer's protocol.

2.3.5 Data correction and analysis

The software CytExpert (Beckman Coulter) was used for the analysis of initial flow cytometry data. To ensure that only viable cells were included in further analysis, cells were additionally stained with the viability dyes 7AAD and FVD. Cells positive for either of these dyes were excluded from further analysis by the appropriate gating. This allowed the calculation of a median fluorescence intensity (MFI) relating to MICA/B ligand expression for each sample. Preliminary experiments showed that unstained cells also emit fluorescence and thus return a raised MFI. We found that this "autofluorescence" was different depending on the cell line and which treatment the cells had undergone. This phenomenon affects the MFI of stained cells and results in too high, inaccurate MFI outputs. Therefore, for each timepoint and treatment group, we determined the MFI of unstained cells. The MFI of these unstained cells was then subtracted from the MFI of stained cells. This way, all fluorescence registered by the flow cytometer can be attributed to the fluorophores tagging the ligands of interest. Once MFIs had been corrected for autofluorescence, the software GraphPad Prism (GraphPad Software) was used to visualise and statistically analyse the data.

3 Results

3.1 MKN28 Cells infected with wild-type *H.pylori* show a higher mRNA expression of MICA/B, ADAM17, and IL-15

To elucidate whether our hypothesis is valid, we initially measured the mRNA expression of the genes MICA, MICB, IL-15, and ADAM17 in MKN28 cells which had been infected with WT P12 strain of *H.pylori* using qPCR. As a control we measured mRNA expression of the same genes in uninfected cells. The CFU controls done at 2, 4, and 6h showed a steadily increasing bacterial load. However, after 24h the bacteria were no longer culturable on agar plates (Fig. 4A). Photomicrographs were made of the cells to assess morphological discrepancies. The cells infected with the WT *H.pylori* strain showed clear signs of cell stress such as vacuolisation, increased apoptosis, and necrosis (Fig. 4B). RNA isolation was done after 2, 4, 6, 24, and 48 hours. MICA and MICB expression in infected cells at the 24h and 48h timepoints was significantly increased compared to the control cells at the 0-hour timepoint (Fig. 4C and D). However, this phenomenon could not be observed at earlier time points. The same can be said for the expression of ADAM17 which was also only increased compared to controls at later timepoints (Fig. 4E). It should be mentioned that while there was an increase in ADAM17 expression, this increase was not as pronounced as with MICA/B. Regarding the expression of IL-15, a significant increase in gene expression compared to the 0h controls could be found at all timepoints except at 2h (Fig. 4F).

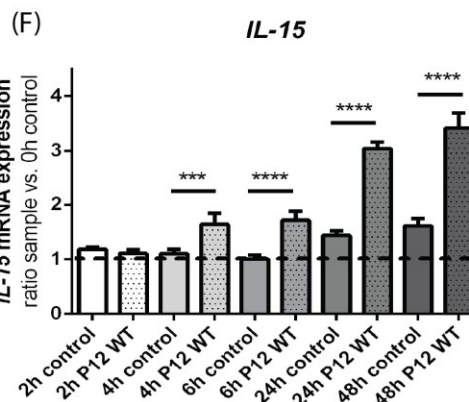
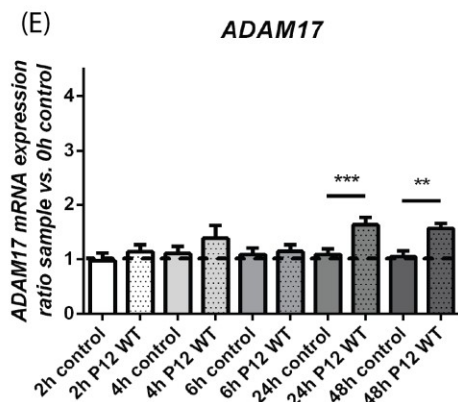
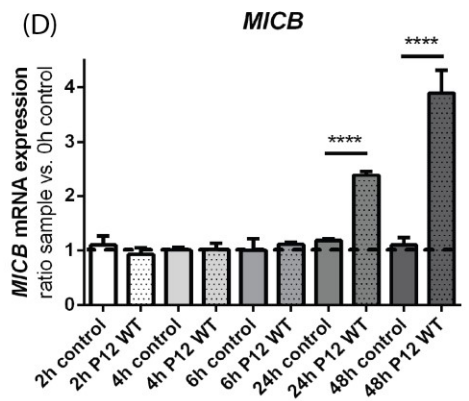
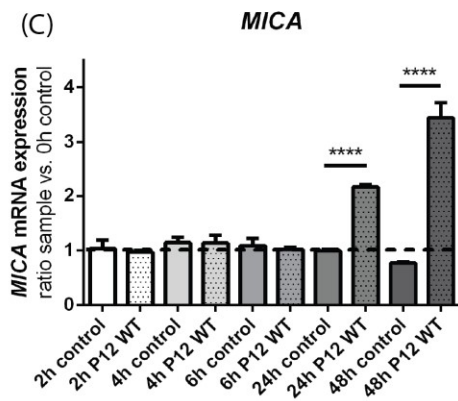
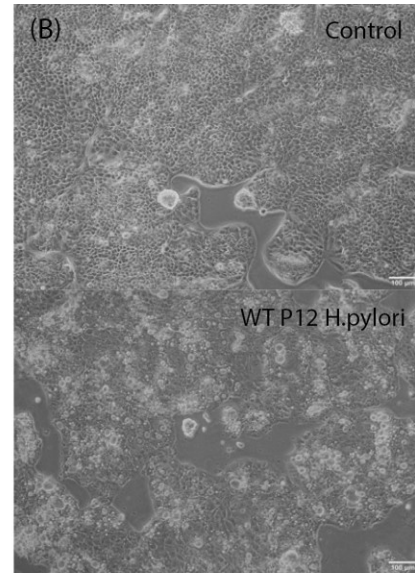
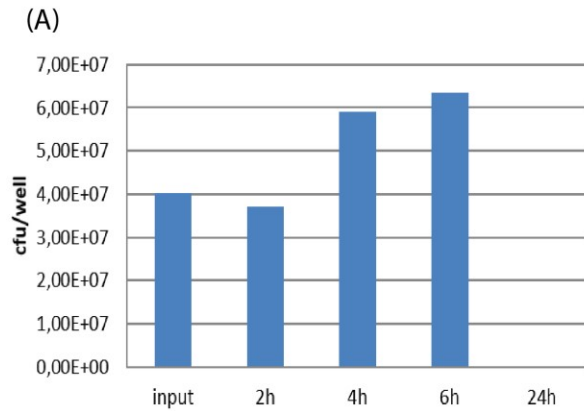


Figure 6: (A) The CFU per well of WT P12 *H.pylori* infected MKN28 cells at different measurement timepoints. Infection was initiated at MOI 50. (B) Photomicrographs of control MKN28 cells and MKN28 cells infected with WT P12 *H.pylori* after 48h. (C-F) mRNA expression of MICA, MICB, IL-15, and ADAM17 in MKN28 cells after 2, 4, 6, 24, and 48 hours of infection with *H.pylori* P12 WT. The results are represented as the ratio of the mRNA expression of each sample versus the mRNA expression of control cells at 0h. Statistical significance was ascertained using one-way ANOVA and Sidak's multiple comparisons test. ** $p < 0,01$; *** $p < 0,001$; **** $p < 0,0001$.

3.2 AGS cells treated with *H.pylori* WT and CagL knockout exhibit a non-significant increase of extracellular MICA/B

AGS cells were cultured and subsequently infected with either WT P12 *H.pylori* or a CagL isogenic knockout strain (Δ CagL). As a control, a fraction of AGS cells were left uninfected and assessed at the same timepoints. CFU controls were done at 24 and 48h. These showed a decreasing bacterial load over time. The Δ CagL strain seemed to be especially aggrieved, as after 48h, it was hardly re-culturable. Samples were also taken and transferred to agar plates for cultivation at the timepoint of infection. Unfortunately, no bacterial colonies grew making it impossible to assess initial bacterial load. Cells were assessed for surface (=extracellular) MICA/B ligand expression after 48h. As expected, control cells expressed the lowest amount of MICA resulting in the lowest median fluorescence intensity (MFI). Interestingly the Δ CagL strain induced greater MICA/B surface expression in treated AGS cells than the WT *H.pylori* strain did. However, these differences were not statistically significant (Fig. 5C).

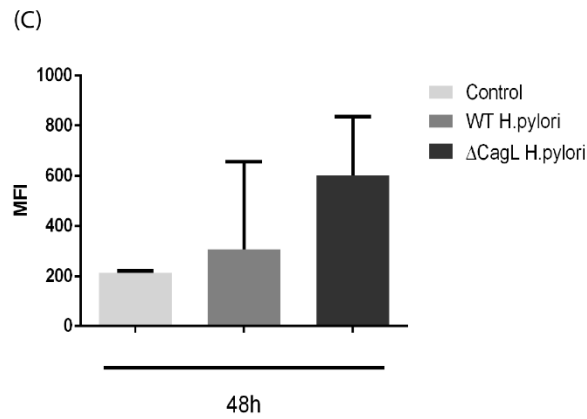
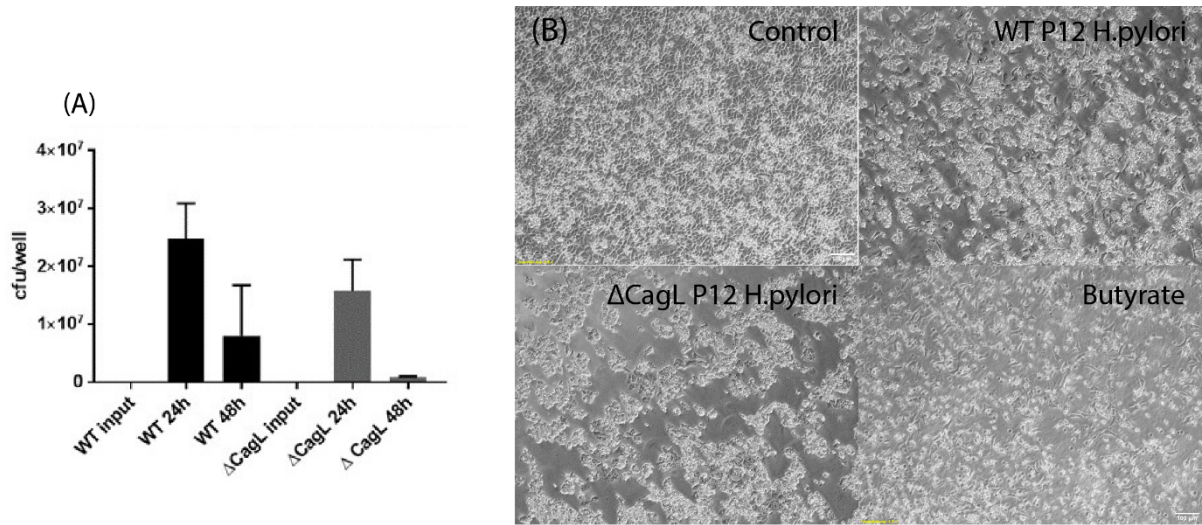


Figure 7: (A) The CFU per well of WT and Δ CagL P12 H.pylori infected AGS cells at different measurement timepoints (MOI 50). (B) Photomicrographs of AGS cells 48 hours after beginning corresponding treatment. (C) Flow cytometric analysis of the extracellular MICA/B ligand expression of AGS cells after infection with H.pylori P12 WT and P12 Δ CagL. Control cells were left untreated. Data represent the MFI of cells stained with an antibody targeting MICA and MICB. To account for cell auto-fluorescence, the MFI of corresponding unstained cells was subtracted. Non-viable cells were excluded from the analysis via 7-AAD or FVD staining.

3.3 HeLa cells treated with butyrate had a significantly increased MIC ligand expression compared to controls

HeLa cells were cultured and subsequently infected with either WT P12 *H.pylori* or a CagL knockout strain. Furthermore, as it is known that butyrate is a strong MIC ligand inducer, cells were treated with butyrate as a positive control. Control samples expressed the least surface MIC ligands. Conversely, the infected HeLa cells showed an opposite trend to that previously observed in AGS cells. *H.pylori* P12 WT infected cells expressed greater amounts of surface MIC ligands than cells infected by the Δ CagL mutant strain. However, both were not significantly increased compared to control cells and both did not differ significantly from each other. MIC ligand expression in control cells increased between the 24 and 48h timepoint. Interestingly, this was not the case for infected cells: The cells infected with WT P12 *H.pylori* showed a minimal increase in MFI and cells infected with the CagL knockout strain prompted a decrease in MFI between the two timepoints. HeLa cells treated with butyrate showed a significantly increased MIC ligand surface expression compared to controls ($p < 0.05$) Interestingly, Dunn's multiple comparisons test revealed that only the 24h butyrate timepoint differed significantly from its respective control (Fig. 6C). Two separate flow cytometric assays were done with HeLa cells. As no unstained cells were measured in the first flow cytometer assay, the MFI of unstained cells from the second assay was used to account for cell auto-fluorescence in the first assay's results. As there are only incomplete measurement points from the first HeLa assay (only 24h timepoint, no overall expression) we opted to combine both experiments and found that the same results could be shown with greater statistical significance. The results from both experiments are depicted in Fig. 6D.

We wanted to additionally assess the internal (=intracellular) expression of MIC ligands. Unfortunately, the process of "cleaving" surface ligands before permeabilization as described in chapter 2.3.3 was not possible with this cell line. This meant that we could not be sure that a signal solely originated from the intracellular stained ligands. We therefore opted to assess the "overall" expression by harvesting the cells in an identical manner to the cells for "surface staining". These cells were stained twice: once extracellularly and once intracellularly after permeabilization. The acquired results were

largely the same as for cells which were stained solely extracellularly. As expected a general increase in MFI could be seen universally in all treatments and timepoints. Similar phenomena regarding MFI alterations between observation timepoints became more prominent, although they remained statistically insignificant. As observed in extracellularly stained cells, butyrate treated cells showed a pronounced increase in MFI between 24 and 48h. However, the additional intracellular staining revealed an even more pronounced change. Again, the only statistically significant increase was observed between HeLa cells treated with butyrate at 24h and their respective control cells (Fig 6E). It should furthermore be mentioned that compared to the other cell lines used in this thesis, HeLa cells' MIC ligand expression was immense. Even untreated HeLa control samples presented an MFI which was over 150 times greater than that of AGS controls.

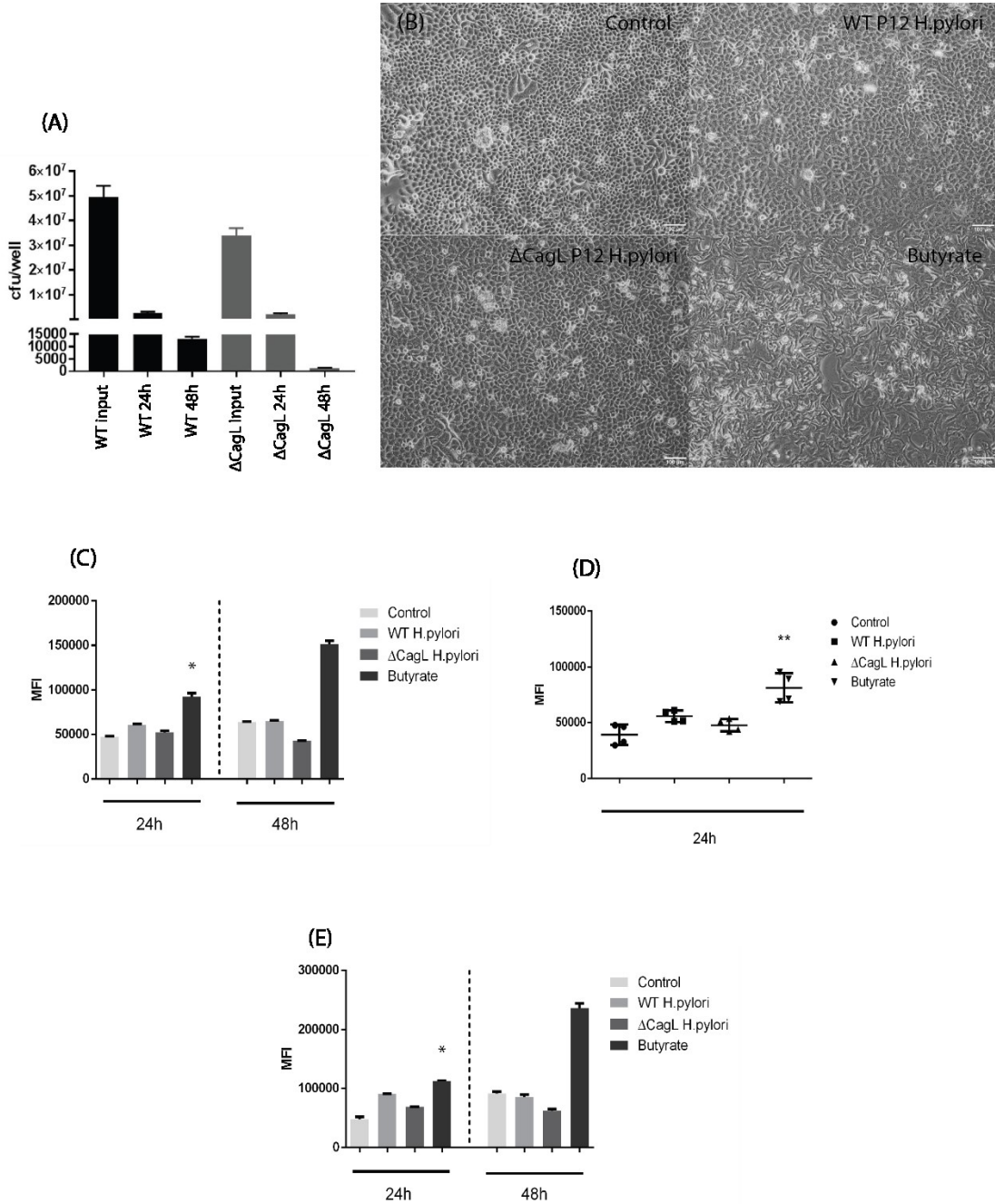


Figure 8: (A) The CFU per well of WT (MOI 75) and Δ CagL (MOI 52) P12 H.pylori infected HeLa cells at different measurement timepoints of the second HeLa infection assay. (B) Photomicrographs of HeLa cells 48 hours after beginning corresponding treatment. Flow cytometric analysis of the extracellular (C) and overall (E) MICA/B expression of HeLa cells after infection with P12 WT and P12 Δ CagL H.pylori or stimulation with butyrate. Control cells were left untreated. (D) Combined measurements of two separate flow cytometry assays measuring extracellular MICA/B ligand expression of HeLa cells after 24h under the same conditions as described above. Data represent the MFI of cells stained by an antibody targeting MICA and MICB. To account for cell auto-fluorescence, the MFI of corresponding unstained cells was subtracted. Non-viable cells were excluded from the analysis via 7-AAD or FVD staining. Statistical significance was ascertained using Kruskal-Wallis' test and Dunn's multiple comparisons test. * $p < 0.05$ compared to respective control samples.

3.4 MKN74

As with the HeLa cell line, two separate assays were performed with MKN74. We considered pooling the results to achieve a larger n-number and higher statistical significance. However, we finally decided against such an approach as the results differed too greatly between the 2 assays; rendering it pointless to compare the results. Therefore, the two assays will be shown separately.

3.4.1 WT P12 *H.pylori* prompts increased MIC ligand expression in MKN74 cells

MKN74 cells were cultured and subsequently infected with either WT P12 *H.pylori* or a CagL knockout strain. CFU controls were done at 24 and 48h. While the Δ CagL strain was not re-culturable at all, the WT strain multiplied quickly between infection and the 24h timepoint. However, after 48h this strain had also become unculturable from assay samples (Fig. 7A). Cells infected with the WT strain showed the most pronounced, yet not statistically significant increase in MIC ligand expression compared to control samples. Photomicrographs of these cells after 48h also indicated serious cell stress and increased cell death (Fig. 7B) The Δ CagL strain seemingly prompted no response as infected cells expressed MIC ligands similarly to control cells. When inspecting these cells morphologically in photomicrographs, the cells infected with the knock-out strain closely resembled control cells (Fig. 7B). Extracellularly stained cells expressed fewer MIC ligands than cells which were stained intracellularly, with intracellularly stained cells reaching an MFI of up to 7000. When comparing the ratios between treatment groups, extra- and intracellular MIC ligand expression was similar at all timepoints. Cells infected with the WT strain consistently expressed the highest number of MIC ligands. Furthermore, extracellular expression of MIC ligands increased drastically between the 24 and 48h timepoints. In contrast, intracellular expression only increased marginally (Fig. 7C-D).

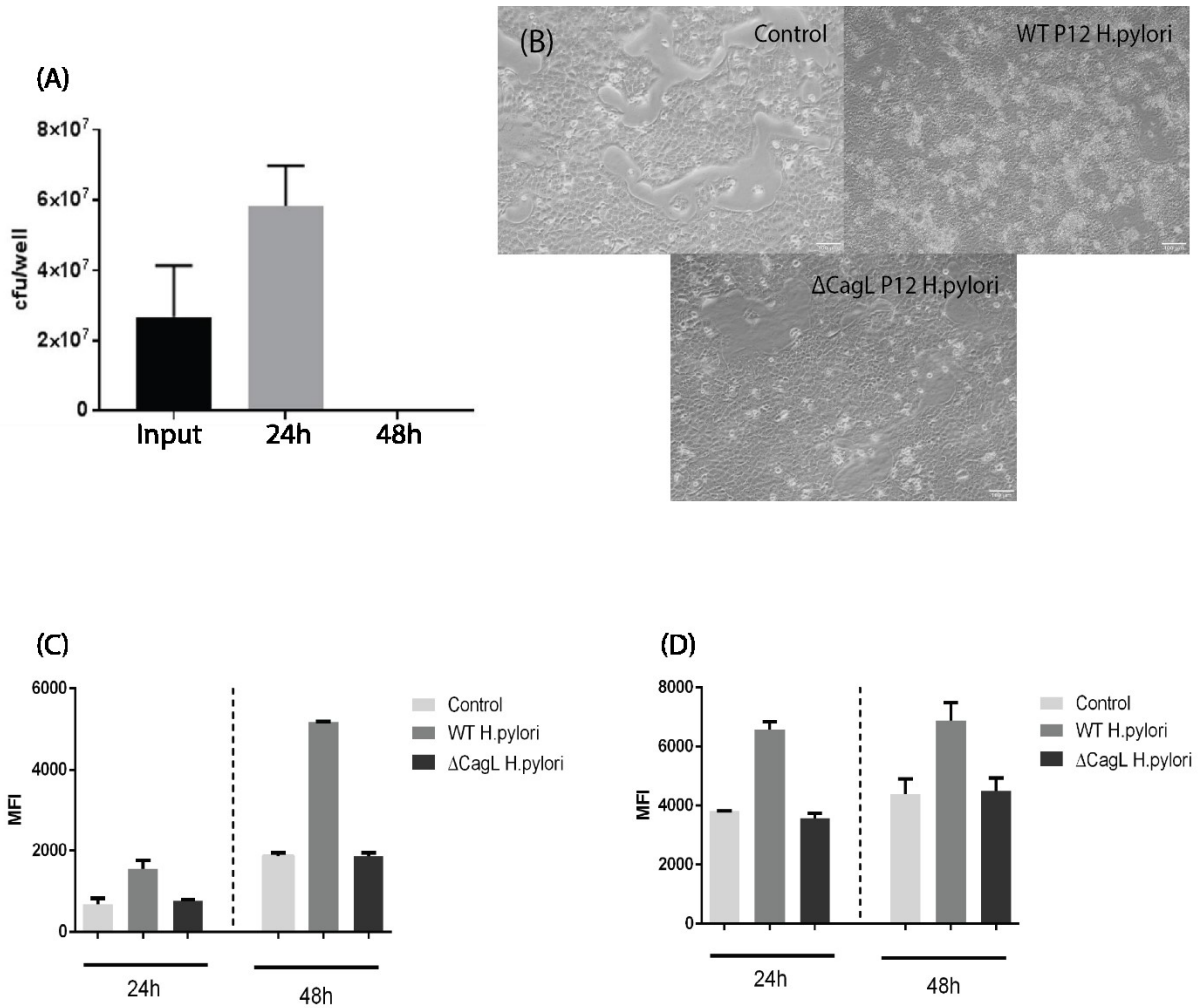


Figure 9: (A) The CFU per well of WT P12 H.pylori infected MKN74 cells at different measurement timepoints (MOI 30). (B) Photomicrographs of MKN74 cells 48 hours after beginning corresponding treatment. Flow cytometric analysis of the extracellular (C) and intracellular (D) MICA/B ligand expression of MKN74 cells after infection with P12 WT and P12 ΔCagL H.pylori. Control cells were left untreated. Data represent the MFI of cells stained with an antibody targeting MICA and MICB. To account for cell auto-fluorescence, the MFI of corresponding unstained cells was subtracted. Non-viable cells were excluded from the analysis via 7-AAD or FVD staining.

3.4.2 MIC ligand expression of MKN74 cells after 48h stimulation with butyrate is significantly increased vs. controls

MKN74 cells were cultured and subsequently infected with either WT P12 *H.pylori* or the CagL knockout mutant. CFU controls were done at 24 and 48h. Both strains remained culturable at every timepoint. However, the CFU declined the longer they remained in contact with the cells. The Δ CagL strain's CFU made a rapid decline between 24 and 48h (Fig. 8A). In this assay, MKN74 cells stimulated with butyrate were used as a positive control. These cells presented by far the highest expression of MIC ligands in both extra- and intracellularly stained cells. However, the only cells which showed a statistically significant increase compared to their respective controls were extracellularly stained cells treated with butyrate at 48h. Control cells always expressed the lowest number of MIC ligands. Whereby their surface MICA/B expression even decreased between 24 and 48h – a phenomenon which was not observed in the previous assay with MKN74 cells. When comparing the cells infected with the two *H.pylori* strain variants, it is evident that the WT induces greater MIC ligand expression. At 24h, the WT infected cells show a surface expression twice as large as cells infected with the Δ CagL strain. This disparity could not be observed when assessing the internal expression. At 48h, extracellular expression of MIC ligands in WT infected cells remained at a similar level to the respective 24h timepoint while the Δ CagL infected cells' MIC ligand expression increased only marginally. No statistically significant differences between infected cells and controls could be found.

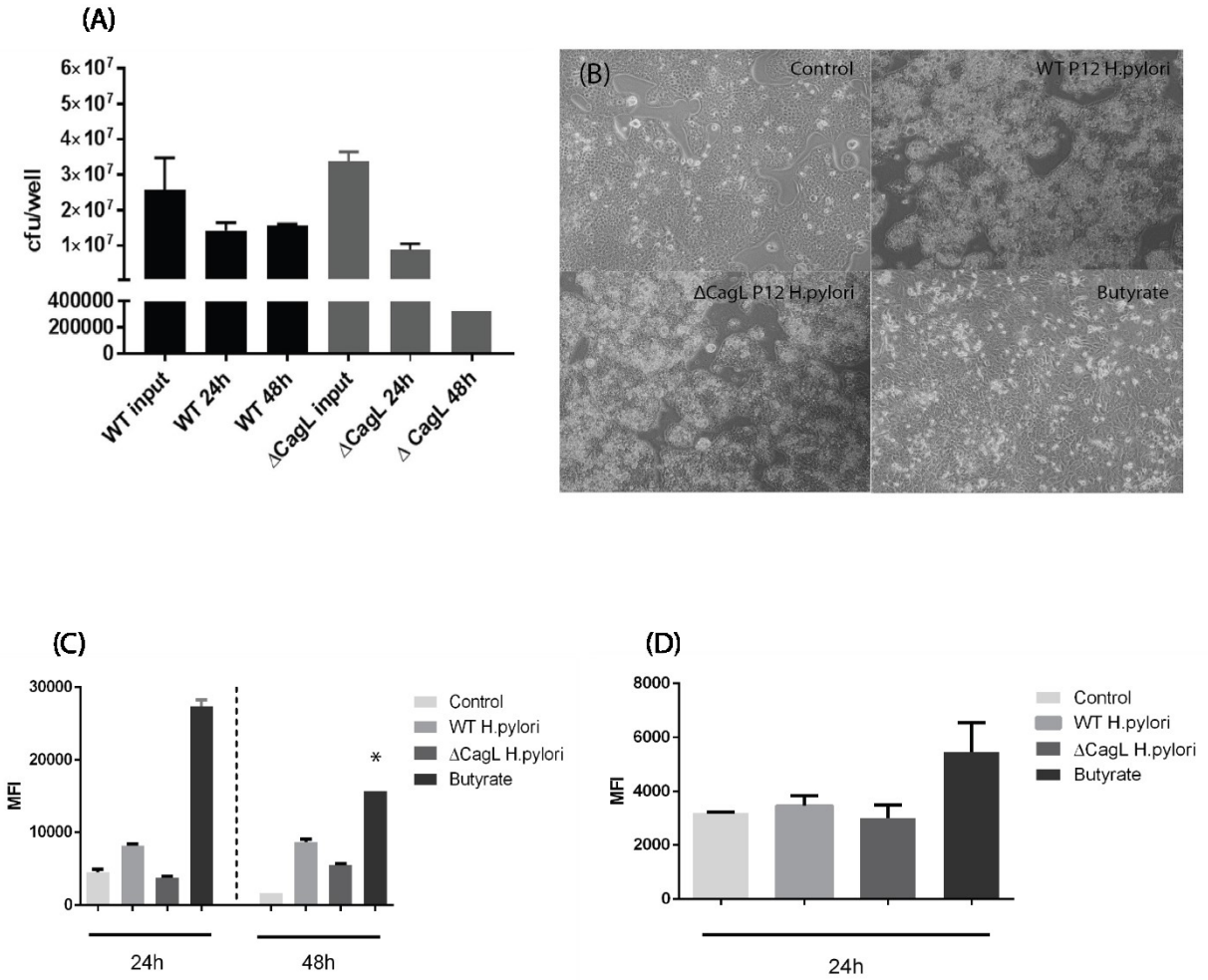


Figure 10: (A) The CFU per well of WT (MOI 35) and Δ CagL (MOI 45) P12 *H.pylori* infected MKN74 cells at different measurement timepoints. (B) Photomicrographs of MKN74 cells 48 hours after beginning corresponding treatment. Flow cytometric analysis of the extracellular (C) and intracellular (D) MICA/B ligand expression of MKN74 cells after infection with WT and Δ CagL P12 *H.pylori* or stimulation with butyrate. Control cells were left untreated. Data represent the MFI of cells stained with an antibody targeting MICA and MICB. To account for cell auto-fluorescence, the MFI of corresponding unstained cells was subtracted. Non-viable cells were excluded from the analysis via 7-AAD or FVD staining. Statistical significance was ascertained using Kruskal-Wallis' test and Dunn's multiple comparisons test. * $p < 0.05$ compared to respective control samples.

4 Discussion

To this day, *Helicobacter pylori* remains one of the most elusive bacteria known to man. It can persist for decades in the stomach of humans. This is certainly made possible by its exceptional adaptation to its ecological niche, the human stomach. For bacteria to achieve infections of such extreme longevity, bacteria must develop mechanisms with which they can elude the host immune system. While the bacterium's entire genome has been sequenced, and many of its virulence factors have been identified, in many ways it has remained an enigma.

Whilst conducting research for her PhD, our colleague A. Montalban-Arques began investigating the human NKG2D receptor. She was assaying biopsies from patients with various gastric maladies and it was then that she observed that the NKG2D receptor was expressed equally or less in patients suffering from *H.pylori* gastritis than healthy controls. This was an observation which at first made no sense at all. NKG2D is known as a receptor which activates the immune system by recognizing induced-self proteins on stressed, malignant, and infected cells. Thus, logical reasoning would suggest that it should be expressed more in tissues which are infected by a pathogen to ensure for an adequate immune response. It was this rationale which led us to the notion that this may well be one of *H.pylori*'s immune escape mechanisms at play. It was therefore that we began looking at existing literature regarding this matter. We found that soluble MIC ligands have been shown to lead to receptor downregulation in cancer patients (89). We reasoned that a possible perpetrator leading to the shedding of these ligands is the matrix metalloproteinase ADAM17 as it has been shown to be implicated in the shedding of NKG2D ligands (94,95). With this thesis we attempted to confirm or refute our hypothesis.

We employed an *in vitro* approach to test our hypothesis as this allowed us to precisely control the infection conditions such as the infecting agent and duration of infection. Furthermore, it allowed us to employ certain techniques more easily, such as flow cytometry, to elucidate current ligand expression of infected cells. We used several gastric cell lines, of which AGS and MKN28 are well known, established cell lines which have been used in numerous publications. The use of such immortalized cell lines is

highly convenient due to their high replication rate, resilience, and facile cultivation. However, it is important to note that there are also negative aspects to working with such cell lines. These cells are derived from malignant tumors. This means that they have sustained mutations, rendering them immortal and allowing them to grow quickly and invasively. This rapid growth makes it possible to grow vast numbers of cells in a comparatively short time; saving time and money. This practicality comes at a price as rapid multiplication inevitably leads to further mutations. These mutations may affect insignificant genes and therefore have no effect. Yet it is equally possible that they affect genes implicated in the mechanism that is being investigated. One should keep this in mind when attempting to interpret the results of assays done with such cell lines. These problems could potentially be overcome by using primary cell lines derived directly from healthy gastric mucosa. These cells would certainly be better suited for studying cellular mechanisms as they are not mutated. However, such cell lines are much more difficult to work with as they grow far more slowly and because they are not immortalized will not divide infinitely. Another, more sophisticated, possibility would be to employ a relatively new technique called organoid cultures. These are 3-dimensional cell cultures which more closely mimic the corresponding organ they are derived from. These organoids can potentially incorporate key features of the represented organ and so serve as a model which more closely resembles an *in vivo* situation. Again, the drawback to this method is the complexity of the approach. In fact, protocols for organoid cultures are far more complex than those required for primary cell culture. Several months of training would be necessary to properly master this technique. At any rate, if one were to employ either of these techniques it would be essential that before any actual lab work is done, a thoroughly thought out project plan is put together. This way one could on the one hand better evaluate which method would be more suitable and on the other hand ensure that one will receive truly meaningful results.

Our assay with the gastric epithelial cell line MKN28 showed that the infection with WT P12 strain of *H.pylori* led to a significantly increased expression of MICA and MICB ligands on a mRNA level; although this effect only became apparent after 24h. Furthermore, the same can be said for ADAM17 mRNA expression, which was also significantly increased at these timepoints. IL-15 mRNA expression was also examined,

and we found a significant increase in expression at 6, 12, 24, and 48h, indicating a strong effect. While these results are not exactly what we were expecting, they certainly do not rule out our hypothesis. It is plausible that in vivo this increased RNA expression would lead to an increased ligand expression. It is also reasonable to assume that an increased number of MIC ligands combined with an increased ADAM17 expression would result in more sMIC ligands being shed from the epithelial cells – resulting in a stronger NKG2D dampening effect. However, an increased mRNA expression cannot be directly equated to an increased ligand expression on the cell surface; which would be necessary for increased ligand shedding. Transcription and post-translational protein processing could be hindered meaning that the ligands are simply never created. Moreover, if anything should interfere with intracellular protein trafficking, the fully functional ligands would never make it to the cell surface – rendering them functionally nonexistent. Unfortunately, this infection assay was only done with the WT *H.pylori* strain. It would be interesting to see how the cells react to a knockout *H.pylori* strain as this would allow to confirm or rule out the involvement of a certain virulence factor.

The increased IL-15 mRNA expression is not as easily explained by our hypothesis. Its key role in inflammatory processes and the differentiation of NK cells, means that it would lead to a proinflammatory environment. It has furthermore been observed that IL-15 directly upregulates and primes the NKG2D receptor (96,97). When regarding A. Montalban-Arques' findings showing a decreased NKG2D receptor expression in gastric biopsies from people suffering from *H.pylori* gastritis, this does not make sense at all. Yet it is possible that other mechanisms are at play which inhibit NKG2D expression to such an extent that the IL-15 induced NKG2D upregulation is annulled. Furthermore, it is possible, especially when considering the sheer longevity of most *H.pylori* infections, that we are simply looking at a timeframe which does not depict the reality of an in vivo infection. Perhaps, IL-15 is downregulated at a later timepoint or other factors come into play which are missing in an in vitro setting.

Next, to address our questions regarding true functional ligand expression we decided to assess gastric epithelial cell lines employing flow cytometry. We opted to use other

gastric cell lines to ensure we receive a broader picture. Our first assay was done using the gastric cell line AGS which is arguably the best known and most studied gastric cell line in the context of *H.pylori* infection. The cells were infected with both the WT as well as CagL knockout P12 *H.pylori* strains. The only timepoint at which flow cytometric analyses were done with AGS cells was at 48h. We found that the Δ CagL strain was the strongest inducer of surface MIC ligand expression. However, there was no statistically significant difference between the different treatments. This can partly be attributed to the fact that we received measurements with large standard deviations (SDs). This experiment would have to be repeated to make sure these findings are accurate and conceivably receive significant results. Should we receive a similar outcome, these findings would strongly support our hypothesis. The fact that the WT strain, which in theory should be more pernicious, induces a lower expression of MIC ligands than the CagL knockout, would indicate strongly that the WT strain is able to reduce extracellular MIC ligand expression and that the protein CagL is necessary. However, the surface MIC ligand expression in cells treated with the WT strain is still greater than in control cells. Moreover, as previously mentioned, the results from the cells infected with both strains are highly imprecise with large SDs. In reality, this makes it impossible to deduce anything from these results with reasonable certainty.

The next cell line with which we did flowcytometric analyses was the world-renowned HeLa cell line. It may at first seem somewhat nonsensical to use cells originating from a cervical carcinoma to study the effects of a gastric pathogen. However, this cell line has previously been shown to exhibit strong expression of NKG2D ligands (98,99). We therefore reasoned that on the one hand it could function as a type of positive control and on the other, that high overall ligand expression may result in even small expression alterations becoming more prominent and significant.

It did not come as a surprise that the group treated with butyrate expressed by far the greatest amount of MIC ligands, as this has been previously described in various publications (100,101). This gave us valuable insight as it showed how a strong ligand induction would present itself. Interestingly, compared to the AGS cells, HeLa cells seemed to exhibit an opposite phenomenon when exposed to the two *H.pylori* strains.

Flowcytometric analysis of the surface MIC ligands showed similar levels of extracellular and overall ligand expression in the group treated with the WT *H.pylori* strain after 48h than what we had measured in control cells. At this timepoint, the CagL knockout treated group expressed less MIC ligands than both these groups. One could reason that the knockout strain induces a reduced expression compared to the WT as its loss of CagL makes it less malicious. This however would not explain it resulting in an expression less than the control group. Moreover, this does not make sense when considering our hypothesis as we expected that the WT strain would reduce MIC ligand expression via the T4SS, a multi-protein structure in which CagL plays a constitutive role. Nonetheless, it is important to keep in mind that these variations concerning the control group and both infected groups are statistically insignificant and small compared to the induction resulting from butyrate treatment. Furthermore, HeLa is, as mentioned before, a cell line which originated from a cervical carcinoma. While it is also an epithelial cell line, it is derived from an organ which fulfils a very different purpose and possesses epithelia which are well adapted to a very different environmental niche. Additionally, because it is such a broadly used cell line it has most certainly been passaged so often that it would be impossible to estimate a passage number – possibly allowing the introduction of numerous mutations. It would therefore be dangerous to assume that our measurements accurately portray the physiological in vivo response of the human gastric mucosa to the bacteria.

We finally did an infection assay with the cell line MKN74; a cell line derived from a gastric adenocarcinoma metastasis. As mentioned in the results, we did two separate assays which were not comparable despite the fact that the same assay protocol was used. In the first assay we found that the WT *H.pylori* strain led to the greatest induction of NKG2D ligands. When regarding the extracellular expression, the difference in ligand expression increases drastically in WT treated cells between the 24h and 48h timepoints. Meanwhile, control and Δ CagL treated cells remain at similar levels. At this point it is important to mention that the Δ CagL strain was not culturable at any of the timepoints. In contrast, the intracellular expression of all treatment groups only changed marginally between the two timepoints. This may indicate that the increase in surface

expression is mediated by an increased production of new ligands rather than delivery of prefabricated intracellular ligands to the cell surface.

As previously mentioned, the second assay included cells stimulated with the SCFA butyrate. Unsurprisingly, these cells showed the greatest MIC ligand expression. While the disparity visually seems greatest at 24h in extracellularly stained cells, the only significant increase compared to controls was at 48h in extracellularly stained cells. This may be because the 24h timepoint bore a greater standard deviation. It is also interesting that the surface ligand expression decreases between the 24 and 48h timepoints in control cells and cells stimulated with butyrate. This may possibly be indicative of a ligand shedding mechanism. Though, this would not support our hypothesis as we were expecting to witness such a phenomenon in WT infected cells. It is not possible for us to assess whether this same decrease in ligand expression over time occurs in intracellular ligand expression as we only assessed the cells' intracellular expression after 24h. We do however have the results from our first MKN74 assay where no such phenomenon can be identified when regarding the control cells' ligand expression. When comparing the cells infected with the *H.pylori* strains we find a similar pattern than in our first MKN74 assay as well as the HeLa assays. WT *H.pylori* leads to a greater increase in the expression of MIC ligands than the Δ CagL mutant, though no statistical significance could be found. This again conflicts with our hypothesis as we would have expected to see the WT strain lead to a decrease rather than an increase.

In conclusion, it is clear that our results do not offer enough concise and compelling evidence to prove our hypothesis. The assessment of the mRNA expression in MKN28 cells hinted at the fact that P12 *H.pylori* increases the gene expression of NKG2D ligands MICA and MICB. At the same time, we measured an increase in ADAM17 expression. When viewed separately from other measurements, these two findings provide strong evidence for our theory that MIC ligand shedding in turn leading to the emergence of sMIC finally results in a downregulation of the NKG2D receptor. However, we cannot disregard the fact that IL-15 was upregulated as well. As IL-15 is known to upregulate NKG2D expression, our results suddenly become less clear. If

one then takes our findings from flow cytometric analyses into consideration, the overall picture becomes even more hazy and ambiguous. Our first flow cytometry results, stemming from an infection assay done with the cell line AGS, were relatively promising. Results showed that the CagL knockout mutant induces greater MIC ligand expression than the WT strain; exactly what we had hypothesised. However, the flow cytometric assays done with the cell lines HeLa and MKN74 suddenly showed an opposite trend. In these cells, the WT led to a greater MIC ligand induction than the knockout mutant. While the results from the AGS cells would support our hypothesis, it is more likely that the results from two separate cell lines more closely represent the in vivo physiological reaction to the bacterium. At present, we can say that judging by the results collected in this thesis, it is unlikely that the proposed hypothetical mechanism represents the in vivo response of gastric epithelial cells to *H.pylori*. In research, disproving something can be just as important as proving it. Yet unfortunately, due the obscurity and sparsity of our results we cannot rule out our hypothesis. To do this one would need to repeat all assays we have done under the same conditions. This is the only way to be sure that our results were accurate. It would be important that both qPCR as well as flow cytometry assays are done with the same cell line to obtain a more complete overall picture. The cell supernatants from the infection assays should also be analysed with diagnostic tests assessing the soluble ligands as flow cytometry only gives us insight into the extracellular ligand expression at a certain timepoint. It is possible that if the ligand shedding and ligand production happens at a similar speed we wouldn't see a difference in expression in our flow cytometric analyses. All these factors would have to be carefully considered when setting up another series of experiments to prove or disprove our hypothesis. It is clear that the results presented in this thesis hardly constitute a complete and comprehensive study. This is because many of the presented results stem from the first preliminary experiments which were partly done to establish and perfect new techniques. We deem our results as valuable nonetheless. Instead of portraying the entire picture, this thesis represents a snapshot of a larger study which will continue for several years to come.

5 References

1. Hall JE. Guyton and Hall textbook of medical physiology. 13th ed. Elsevier; 2016. 1145 p.
2. Tennant SM, Hartland EL, Phumoonna T, Lyras D, Rood JI, Robins-Browne RM, et al. Influence of gastric acid on susceptibility to infection with ingested bacterial pathogens. *Infect Immun*. 2008;76(2):639–45.
3. Nwokolo CU, Loft DE, Holder R. Increased incidence of bacterial diarrhea in patients taking gastric acid antisecretory drugs. *Eur J Gastroenterol Hepatol*. 1994;6:697–9.
4. Howden CW, Hunt RH. Relationship between gastric secretion and infection. *Gut*. 1987;28(1):96–107.
5. Linney S, Fernandes T, Einarson T, Sengar A, Walker JH, Mills A. Association Between Use of Proton Pump Inhibitors and a Clostridium difficile-Associated Disease Outbreak: Case-Control Study. *Can J Hosp Pharm*. 2010;63(1):31–7.
6. Dalton BR, Lye-Maccannell T, Henderson EA, MacCannell DR, Louie TJ. Proton pump inhibitors increase significantly the risk of Clostridium difficile infection in a low-endemicity, non-outbreak hospital setting. *Aliment Pharmacol Ther*. 2009;29(6):626–34.
7. Patil R, Blankenship L. Proton Pump Inhibitors and Clostridium Difficile Infection: Are We Propagating an Already Rapidly Growing Healthcare Problem? *Gastroenterol Res*. 2013;6(5):171–3.
8. Aseeri M, Schroeder T, Kramer J, Zackula R. Gastric Acid Suppression by Proton Pump Inhibitors as a Risk Factor for Clostridium Difficile -Associated Diarrhea in Hospitalized Patients. *Am J Gastroenterol*. 2008 Sep;103(9):2308–13.
9. Quigley EMM. Gut bacteria in health and disease. *Gastroenterol Hepatol (N Y)*. 2013;9(9):560–9.
10. Whiteside SA, Razvi H, Dave S, Reid G, Burton JP. The microbiome of the

urinary tract - a role beyond infection. *Nat Rev Urol*. 2015 Feb;12(2):81–90.

11. Grice EA, Kong HH, Renaud G, Grice EA, Kong HH, Renaud G, et al. A diversity profile of the human skin microbiota. *Nat Rev Microbiol*. 2008;10(4):307–16.
12. Avila M, Ojcius DM, Yilmaz O. The oral microbiota: living with a permanent guest. *DNA Cell Biol*. 2009;28(8):405–11.
13. Sonnenburg ED, Smits SA, Tikhonov M, Higginbottom SK, Wingreen NS, Sonnenburg JL. Diet-induced extinctions in the gut microbiota compound over generations. *Nature*. 2016;529(7585):212–5.
14. David LA, Maurice CF, Carmody RN, Gootenberg DB, Button JE, Wolfe BE, et al. Diet rapidly and reproducibly alters the human gut microbiome. *Nature*. 2014;505(7484):559–63.
15. Sekirov I, Russell S, Antunes L. Gut microbiota in health and disease. *Physiol Rev*. 2010;90(3):859–904.
16. Cryan JF, Dinan TG. Mind-altering microorganisms: the impact of the gut microbiota on brain and behaviour. *Nat Rev Neurosci*. 2012;13(10):701–12.
17. Fröhlich EE, Farzi A, Mayerhofer R, Reichmann F, Jačan A, Wagner B, et al. Cognitive impairment by antibiotic-induced gut dysbiosis: Analysis of gut microbiota-brain communication. *Brain Behav Immun*. 2016;57:1–10.
18. Hsiao EY, McBride SW, Hsien S, Sharon G, Hyde ER, McCue T, et al. Microbiota modulate behavioral and physiological abnormalities associated with neurodevelopmental disorders. *Cell*. 2013 Dec 19;155(7):1451–63.
19. Bercik P, Denou E, Collins J, Jackson W, Lu J, Jury J, et al. The intestinal microbiota affect central levels of brain-derived neurotrophic factor and behavior in mice. *Gastroenterology*. 2011 Aug;141(2):599–609, 609-3.
20. Gerritsen J, Smidt H, Rijkers GT, De Vos WM. Intestinal microbiota in human health and disease: The impact of probiotics. *Genes Nutr*. 2011;6(3):209–40.

21. Sender R, Fuchs S, Milo R. Revised Estimates for the Number of Human and Bacteria Cells in the Body. *PLoS Biol.* 2016;14(8):1–14.
22. Vighi G, Marcucci F, Sensi L, Di Cara G, Frati F. Allergy and the gastrointestinal system. *Clin Exp Immunol.* 2008;153(SUPPL. 1):3–6.
23. Suzuki K, Ha S, Tsuji M, Fagarasan S. Intestinal IgA synthesis: A primitive form of adaptive immunity that regulates microbial communities in the gut. *Semin Immunol.* 2007 Apr;19(2):127–35.
24. Liu S, Da Cunha AP, Rezende RM, Cialic R, Wei Z, Bry L, et al. The Host Shapes the Gut Microbiota via Fecal MicroRNA. *Cell Host Microbe.* 2016;19(1):32–43.
25. Lin L, Zhang J. Role of intestinal microbiota and metabolites on gut homeostasis and human diseases. *BMC Immunol.* 2017;18(1):2.
26. Schwechheimer C, Kuehn MJ. Outer-membrane vesicles from Gram-negative bacteria: biogenesis and functions. *Nat Rev Microbiol.* 2015;13(10):605–19.
27. Hengge R, Sourjik V. Bacterial regulatory networks--from self-organizing molecules to cell shape and patterns in bacterial communities. *EMBO Rep.* 2013;14(8):667–9.
28. Marshall BJ, Warren JR. Unidentified Curved Bacilli in the Stomach of Patients With Gastritis and Peptic Ulceration. *Lancet.* 1984;323(8390):1311–5.
29. Bik EM, Eckburg PB, Gill SR, Nelson KE, Purdom EA, Francois F, et al. Molecular analysis of the bacterial microbiota in the human stomach. *Proc Natl Acad Sci U S A.* 2006;103(3):732–7.
30. Minalyan A, Gabrielyan L, Scott D, Jacobs J, Pisegna JR. The Gastric and Intestinal Microbiome: Role of Proton Pump Inhibitors. *Curr Gastroenterol Rep.* 2017;19(8).
31. Nielsen JA, Roberts CA, Lager DJ, Putchá R V., Jain R, Lewin M. Lymphocytic Gastritis is not Associated with active *Helicobacter pylori* Infection. *Helicobacter.* 2014;19(5):349–55.

32. Alsaigh N, Odze R, Goldman H, Antonioli D, Ott MJ, Leichtner A. Gastric and esophageal intraepithelial lymphocytes in pediatric celiac disease. *Am J Surg Pathol.* 1996 Jul;20(7):865–70.
33. Montalban-Arques A, Wurm P, Trajanoski S, Schauer S, Kienesberger S, Halwachs B, et al. Propionibacterium acnes overabundance and natural killer group 2 member D system activation in corpus-dominant lymphocytic gastritis. *J Pathol.* 2016;240(4):425–36.
34. Stark RM, Gerwig GJ, Pitman RS, Potts LF, Williams N a, Greenman J, et al. Biofilm formation by Helicobacter pylori. *Lett Appl Microbiol.* 1999;28(2):121–6.
35. Chan WY, Hui PK LK. Coccoid forms of H. pylori in the human stomach. *Am J Clin Pathol.* 1994;102(4):121–6.
36. Leying H, Suerbaum S, Geis G, Haas R. Cloning and genetic characterization of a Helicobacter pylori flagellin gene. *Mol Microbiol.* 1992;6(19):2863–74.
37. Suerbaum S, Josenhans C, Labigne A. Cloning and Genetic-Characterization of the Helicobacter-Pylori and Helicobacter-Mustelae FlaB Flagellin Genes and Construction of Helicobacter-Pylori FlaA-Negative and FlaB-Negative Mutants by Electroporation-Mediated Allelic Exchange. *J Bacteriol.* 1993;175(11):3278–88.
38. Suerbaum S. The complex flagella of gastric Helicobacter species. *Trends Microbiol.* 1995;3(5):168-170-171.
39. Eaton KA, Morgan DR, Krakowka S. Motility as a Factor in the Colonization of Gnotobiotic Piglets by Helicobacter-Pylori. *J Med Microbiol.* 1992;37(2):123–7.
40. Josenhans C, Labigne A, Suerbaum S. Comparative ultrastructural and functional studies of Helicobacter pylori and Helicobacter mustelae flagellin mutants: Both flagellin subunits, FlaA and FlaB, are necessary for full motility in Helicobacter species. *J Bacteriol.* 1995;177(11):3010–20.
41. Clyne M, Ocroinin T, Suerbaum S, Josenhans C, Drumm B. Adherence of isogenic flagellum-negative mutants of Helicobacter pylori and Helicobacter mustelae to human and ferret gastric epithelial cells. *Infect Immun.*

2000;68(7):4335–9.

42. Hogg S. *Essential Microbiology*. 1st ed. John Wiley and Sons; 2005. 91-107 p.
43. Olson JW. Molecular Hydrogen as an Energy Source for *Helicobacter pylori*. *Science* (80-). 2002;298(5599):1788–90.
44. Mobley HL. The role of *Helicobacter pylori* urease in the pathogenesis of gastritis and peptic ulceration. *Aliment Pharmacol Ther*. 1996 Apr;10 Suppl 1:57–64.
45. Agrawal A, Gupta A, Chandra M, Koowar S. Role of *Helicobacter pylori* infection in the pathogenesis of minimal hepatic encephalopathy and effect of its eradication. *Indian J Gastroenterol*. 2011 Feb 18;30(1):29–32.
46. Testerman TL, Morris J. Beyond the stomach: An updated view of *Helicobacter pylori* pathogenesis, diagnosis, and treatment. *World J Gastroenterol*. 2014;20(36):12781–808.
47. Hatakeyama M, Higashi H. *Helicobacter pylori* CagA: a new paradigm for bacterial carcinogenesis. *Cancer Sci*. 2005 Dec 1;96(12):835–43.
48. Parsonnet J, Hansen S, Rodriguez L, Gelb AB, Warnke RA, Jellum E, et al. *Helicobacter pylori* Infection and Gastric Lymphoma. *N Engl J Med*. 1994 May 5;330(18):1267–71.
49. Zhou X, Wu J, Zhang G. Association between *Helicobacter pylori* and asthma. *Eur J Gastroenterol Hepatol*. 2013;25(4):460–8.
50. Zevit N, Balicer RD, Cohen HA, Karsh D, Niv Y, Shamir R. Inverse Association Between *Helicobacter pylori* and Pediatric Asthma in a High-Prevalence Population. *Helicobacter*. 2012;17(1):30–5.
51. Imamura S, Sugimoto M, Kanemasa K, Sumida Y, Okanoue T, Yoshikawa T, et al. Inverse association between *Helicobacter pylori* infection and allergic rhinitis in young Japanese. *J Gastroenterol Hepatol*. 2010;25(7):1244–9.
52. Arnold IC, Dehzad N, Reuter S, Martin H, Becher B, Taube C, et al. *Helicobacter pylori* infection prevents allergic asthma in mouse models through the induction

of regulatory T cells. *J Clin Invest*. 2011;121(8):3088–3093.

53. Lebwohl B, Blaser MJ, Ludvigsson JF, Green PHR, Rundle A, Sonnenberg A, et al. Decreased risk of celiac disease in patients with helicobacter pylori colonization. *Am J Epidemiol*. 2013;178(12):1721–30.
54. Konturek PC, Rienecker H, Hahn EG, Raithel M. Helicobacter pylori as a protective factor against food allergy. *Med Sci Monit*. 2008;14(9):453–9.
55. Miftahussurur M, Nusi IA, Graham DY, Yamaoka Y. Helicobacter, hygiene, atopy, and asthma. *Front Microbiol*. 2017;8.
56. Cullinan P, Harris JM, Taylor AJN, Jones M, Taylor P, Dave JR, et al. Can early infection explain the sibling effect in adult atopy? *Eur Respir J*. 2003;22(6):956–61.
57. Lee SP, Lee SY, Kim JH, Sung IK, Park HS, Shim CS, et al. Correlation between helicobacter pylori infection, IgE hypersensitivity, and allergic disease in Korean adults. *Helicobacter*. 2015;20(1):49–55.
58. Matricardi PM, Rosmini F, Riondino S, Fortini M, Ferrigno L, Rapicetta M, et al. Exposure to foodborne and orofecal microbes versus airborne viruses in relation to atopy and allergic asthma: epidemiological study. *Bmj*. 2000;320(7232):412–7.
59. Palframan SL, Kwok T, Gabriel K. Vacuolating cytotoxin A (VacA), a key toxin for Helicobacter pylori pathogenesis. *Front Cell Infect Microbiol*. 2012;2(July):1–9.
60. Tartaglia M, Mehler EL, Goldberg R, Zampino G, Brunner HG, Kremer H, et al. Mutations in PTPN11, encoding the protein tyrosine phosphatase SHP-2, cause Noonan syndrome. *Nat Genet*. 2001;29(4):465–8.
61. Murata-Kamiya N. Pathophysiological functions of the CagA oncoprotein during infection by Helicobacter pylori. *Microbes Infect*. 2011;13(10):799–807.
62. Backert S, Tegtmeyer N, Fischer W. Composition, structure and function of the Helicobacter pylori cag pathogenicity island encoded type IV secretion system.

- Future Microbiol. 2015;10(6):955–65.
63. Kwok T, Zabler D, Urman S, Rohde M, Hartig R, Wessler S, et al. Helicobacter exploits integrin for type IV secretion and kinase activation. *Nature*. 2007;449(7164):862–6.
 64. Shaffer CL, Gaddy JA, Loh JT, Johnson EM, Hill S, Hennig EE, et al. Helicobacter pylori exploits a unique repertoire of type iv secretion system components for pilus assembly at the bacteria-host cell interface. *PLoS Pathog*. 2011;7(9).
 65. Wiedemann T, Hofbaur S, Tegtmeyer N, Huber S, Sewald N, Wessler S, et al. Helicobacter pylori CagL dependent induction of gastrin expression via a novel $\alpha\beta 5$ -integrin–integrin linked kinase signalling complex. *Gut*. 2012;61(7):986–96.
 66. Tegtmeyer N, Hartig R, Delahay RM, Rohde M, Brandt S, Conradi J, et al. A small fibronectin-mimicking protein from bacteria induces cell spreading and focal adhesion formation. *J Biol Chem*. 2010;285(30):23515–26.
 67. Normanno N, De Luca A, Bianco C, Strizzi L, Mancino M, Maiello MR, et al. Epidermal growth factor receptor (EGFR) signaling in cancer. *Gene*. 2006;366(1):2–16.
 68. Dreux AC, Lamb DJ, Modjtahedi H, Ferns GAA. The epidermal growth factor receptors and their family of ligands: Their putative role in atherogenesis. *Atherosclerosis*. 2006;186(1):38–53.
 69. Sulzmaier FJ, Jean C, Schlaepfer DD. FAK in cancer: mechanistic findings and clinical applications. *Nat Rev Cancer*. 2014;14(9):598–610.
 70. Dehm SM, Bonham K. SRC gene expression in human cancer: the role of transcriptional activation. *Biochem Cell Biol*. 2004;82:263–74.
 71. Black RA, Rauch CT, Kozlosky CJ, Peschon JJ, Slack JL, Wolfson MF, et al. A metalloproteinase disintegrin that releases tumour-necrosis factor- α from cells. *Vol. 385, Nature*. 1997. p. 729–33.

72. Lee AM, Diasio RB. ADAM-17: A target to increase chemotherapeutic efficacy in colorectal cancer? *Clin Cancer Res.* 2010;16(13):3319–21.
73. Mohme M, Riethdorf S, Pantel K. Circulating and disseminated tumour cells — mechanisms of immune surveillance and escape. *Nat Rev Clin Oncol.* 2016;14(3):155–67.
74. Atherton JC, Blaser MJ. Coadaption of *Helicobacter pylori* and humans: ancient history, modern implications. *J Clin Invest.* 2009;119(9):2475–2487.
75. Zhang S, Moss SF. Rodent models of *Helicobacter* infection, inflammation and disease. *Methods Mol Biol.* 2012;921(22):89–98.
76. Moran AP, Lindner B, Walsh EJ. Structural characterization of the lipid A component of *Helicobacter pylori* rough- and smooth-form lipopolysaccharides. *J Bacteriol.* 1997;179(20):6453–63.
77. Cullen TW, Giles DK, Wolf LN, Ecobichon C, Boneca IG, Trent MS. *Helicobacter pylori* versus the host: Remodeling of the bacterial outer membrane is required for survival in the gastric mucosa. *PLoS Pathog.* 2011;7(12).
78. Hock BD, McKenzie JL, Keenan JI. *Helicobacter pylori* outer membrane vesicles inhibit human T cell responses via induction of monocyte COX-2 expression. *Pathog Dis.* 2017;75(4).
79. Lewis ND, Asim M, Barry DP, Sablet T De, Singh K, Piazuolo MB, et al. Immune Evasion by *Helicobacter pylori* is Mediated by Induction of Macrophage Arginase II. *J Immunol.* 2011;186(6):3632–41.
80. Obeidy P, Sharland AF. NKG2D and its ligands. *Int J Biochem Cell Biol.* 2009;41(12):2364–7.
81. Radosavljevic M, Cuillerier B, Wilson MJ, Clément O, Wicker S, Gilfillan S, et al. A cluster of ten novel MHC class I related genes on human chromosome 6q24.2-q25.3. *Genomics.* 2002;79(1):114–23.
82. Eagle R a, Trowsdale J. Promiscuity and the single receptor: NKG2D. *Nat Rev*

Immunol. 2007;7(9):737–44.

83. Tieng V, Le Bouguéne C, du Merle L, Bertheau P, Desreumaux P, Janin A, et al. Binding of Escherichia coli adhesin AfaE to CD55 triggers cell-surface expression of the MHC class I-related molecule MICA. Proc Natl Acad Sci U S A. 2002;99(5):2977–82.
84. Hüe S, Mention JJ, Monteiro RC, Zhang SL, Cellier C, Schmitz J, et al. A direct role for NKG2D/MICA interaction in villous atrophy during celiac disease. Immunity. 2004;21(3):367–77.
85. Allez M, Tieng V, Nakazawa A, Treton X, Pacault V, Dulphy N, et al. CD4+NKG2D+ T Cells in Crohn's Disease Mediate Inflammatory and Cytotoxic Responses Through MICA Interactions. Gastroenterology. 2007;132(7):2346–58.
86. Eagle R a., Jafferji I, Barrow AD. Beyond Stressed Self: Evidence for NKG2D Ligand Expression on Healthy Cells. Curr Immunol Rev. 2009;5(1):22–34.
87. Grabstein KH, Eisenman J, Shanebeck K, Rauch C, Srinivasan S, Fung V, et al. Cloning of a T cell growth factor that interacts with the beta chain of the interleukin-2 receptor. Science. 1994;264(5161):965–8.
88. Pagliari D, Cianci R, Frosali S, Landolfi R, Cammarota G, Newton EE, et al. The role of IL-15 in gastrointestinal diseases: A bridge between innate and adaptive immune response. Cytokine Growth Factor Rev. 2013;24(5):455–66.
89. Groh V, Wu J, Yee C, Spies T. Tumour-derived soluble MIC ligands impair expression of NKG2D and T-cell activation. Nature. 2002;419(6908):734–8.
90. Waldhauer I, Goehlsdorf D, Gieseke F, Waldhauer I, Goehlsdorf D, Gieseke F, et al. Tumor-Associated MICA Is Shed by ADAM Proteases. 2008;6368–76.
91. Huang TZWZM, Chen RFX. Prognostic value of ADAM17 in human gastric cancer. 2012;2684–90.
92. Saha A, Backert S, Hammond CE, Gooz M, Smolka AJ. Helicobacter pylori CagL

- Activates ADAM17 to Induce Repression of the Gastric H, K-ATPase α Subunit. *Gastroenterology*. 2010;139(1):239–48.
93. Schneider S, Carra G, Sahin U, Hoy B, Rieder G, Wessler S. Complex cellular responses of *Helicobacter pylori*-colonized gastric adenocarcinoma cells. *Infect Immun*. 2011;79(6):2362–71.
 94. Raab S, Kropp KN, Steinle A, Klein G, Kanz L, Kopp H-G, et al. Platelet-Derived Proteases ADAM10 and ADAM17 Impair NK Cell Immunosurveillance of Metastasizing Tumor Cells By Diminishing NKG2D Ligand Surface Expression. *Blood*. 2014;124(21).
 95. Maurer S, Kropp KN, Klein G, Steinle A, Haen SP, Walz JS, et al. Platelet-mediated shedding of NKG2D ligands impairs NK cell immune-surveillance of tumor cells. *Oncoimmunology*. 2018 Feb 27;7(2):e1364827.
 96. Bauer S, Groh V, Wu J, Steinle A, Phillips JH, Lanier LL, et al. Activation of NK cells and T cells by NKG2D, a receptor for stress-inducible MICA. *Science*. 1999 Jul 30;285(5428):727–9.
 97. Roberts AI, Lee L, Schwarz E, Groh V, Spies T, Ebert EC, et al. Cutting Edge: NKG2D Receptors Induced by IL-15 Costimulate CD28-Negative Effector CTL in the Tissue Microenvironment. *J Immunol*. 2001;167(10):5527–30.
 98. del Toro-Arreola S, Arreygue-Garcia N, Aguilar-Lemarroy A, Cid-Arregui A, Jimenez-Perez M, Haramati J, et al. MHC class I-related chain A and B ligands are differentially expressed in human cervical cancer cell lines. *Cancer Cell Int*. 2011;11(1):15.
 99. Groh V, Rhinehart R, Secrist H, Bauer S, Grabstein KH, Spies T. Broad tumor-associated expression and recognition by tumor-derived gamma delta T cells of MICA and MICB. *Proc Natl Acad Sci U S A*. 1999;96(12):6879–84.
 100. Zhang C, Wang Y, Zhou Z, Zhang J, Tian Z. Sodium butyrate upregulates expression of NKG2D ligand MICA/B in HeLa and HepG2 cell lines and increases their susceptibility to NK lysis. *Cancer Immunol Immunother*. 2009;58(8):1275–

85.

101. Valés-Gómez M, Chisholm SE, Cassady-Cain RL, Roda-Navarro P, Reyburn HT. Selective induction of expression of a ligand for the NKG2D receptor by proteasome inhibitors. *Cancer Res.* 2008;68(5):1546–54.

6 Appendix

6.1 *H.pylori* agar plates

6.1.1 Ingredients for agar solution

Makes 750ml of agar solution for pouring cultivation plates

Ingredients		Type of strain	
Substance	Manufacturer	<i>H.pylori</i> WT P12 (no antibiotic)	<i>H.pylori</i> Δ cagL (Chloramphenicol)
GC Agar	Oxoid	27g	27g
Proteose-peptone	Millipore Corporation	11.25g	11.25g
Deionised water		667ml	667ml
Vitamin mix	See 6.1.2	7.5ml	7.5ml
Horse serum	Pan Biotech	75ml	75ml
Nystatin	Merck	0.75mg	0.75mg
Trimethoprim	Sigma Aldrich	1.875 mg	1.875 mg
Chloramphenicol	Sigma Aldrich	-	4.5 mg

Table 2: Ingredients for agar plates

Mix deionised H₂O with CG Agar and Proteose-peptone and autoclave them. When cooled to ~60°C add the remaining ingredients, mix thoroughly, and pour plates quickly before the agar hardens.

6.1.2 Vitamin mix for agar *H.pylori* agar plates

Dissolve in 500ml of deionised H ₂ O		
Substance	Manufacturer	Amount
Dextrose	Sigma	100 g
L-Glutamine	Sigma	10 g
L-Cysteine	Serva	26 g

Carboxylase	Sigma	100 mg
Fe (NO ₃) ₃	Fluka	20 mg
Vitamin B1 hydrochloride	Serva	3 mg
p-aminobenzoic acid	Sigma	13 mg
DPN/NAD	Sigma	150 mg
Vitamin B12	Sigma	10 mg

Table 3: Vitamin mix – first of 2 solutions.

Dissolve in 300ml of deionised H₂O and 15ml 32% HCL		
Substance	Manufacturer	Amount
L-Cystein	Sigma	1.1 g
Adenine	Sigma	1 g
Guanine	Fluka	30 mg
Arginin	Merck	150 mg
Uracil	Sigma	0.5 g

Table 4: Vitamin mix – second of 2 solutions.

Make both solutions separately. Stir well until completely dissolved then combine both solutions. Finally fill up to 1L with deionised H₂O and sterile filter the solution. Aliquot into 50 ml tubes and store at -20°C.

6.2 qPCR primers

Gene name	Abbreviation	GenBank Accession No.	Primer orientation	Sequence (5' to 3')
Beta actin	ACTB	NM_001101	F	CGTGCTGCTGACCGAGG
			R	ACAGCCTGGATAGCAACGTAC
	GAPDH	NM_002046	F	cccttcattgacctcaactacatg

Glyceraldehyde 3-phosphate dehydrogenase			R	tgggatttccattgatgacaagc
MHC class I polypeptide-related sequence A	MICA	NM_000247	F	AGCCGCTGAGAGGGTGG
			R	GAAGATGCCAGCCAGAAGCA
MHC class I polypeptide-related sequence B	MICB	NM_005931	F	CACCTGCTACATGGAACACAGC
			R	ACATGGAATGTCTGCCAATGATC
Interleukin 15	IL15	unpublished	F	CATGTCTTCATTTTGGGCTGT
			R	GGGTGAACATCACTTTCCGT
ADAM metalloproteinase domain 17	ADAM17	NM_003183	F	GTGGATGGTAAAAACGAAAGCG
			R	GGCTAGAACCCTAGAGTCAGG
			R	ACGTCRTCCCCACCTTC
			R	TGGACCTGCAAGTAAAATCCC

Table 5: qPCR primers used in this thesis

6.3 qPCR standard curve protocol

The cDNA concentrations used to create the standard curves were 20, 4, 0.8, 0.16, 0.032, and 0.0064 ng/well.

The cDNA used was pooled from various control and infected samples from previous experiments. The corresponding amount of cDNA, solved in 4µl ultra-pure deionised water. 6µl of master mix was used per reaction; whereby the master mix was comprised of 5µl of SYBR Green PCR master mix (Applied Biosystems) and 0.5µl of both forward and reverse primers at the above stated concentrations solved in ultra-pure deionised water.